energies

MDPI

Article

Suitability Analysis of Selected Methods for Modelling Infrasound and Low-Frequency Noise from Wind Turbines

Bartłomiej Stępień *, Tadeusz Wszołek, Dominik Mleczko, Paweł Małecki, Paweł Pawlik, Maciej Kłaczyński and Marcjanna Czapla

Department of Mechanics and Vibroacoustics, Faculty of Mechanical Engineering and Robotics, AGH University of Krakow, al. A. Mickiewicza 30, 30-059 Krakow, Poland; twszolek@agh.edu.pl (T.W.); pawel.malecki@agh.edu.pl (P.M.); pawlik@agh.edu.pl (P.P.); mczapla@agh.edu.pl (M.C.)
* Correspondence: bartlomiej.stepien@agh.edu.pl

Abstract: Wind turbines emit infrasound and low-frequency noise (ILFN), which can be annoying for people living near wind farms. To assess the acoustic impact of wind turbines on the environment, it is essential to model ILFN propagation during the forecasting stage. This study assesses the effectiveness of three commonly used sound propagation models (ISO 9613-2, CNOSSOS-EU for favourable propagation conditions, Nord2000) in predicting ILFN generated by wind turbines. The performance of these models in modelling ILFN is generally not validated or guaranteed. The analysis covers octave frequency bands ranging from 4 Hz to 250 Hz, and comparisons are made against measurements conducted at a wind farm in Poland. Non-parametric statistical tests were used with a significance level of $\alpha = 0.05$ to determine significant differences between measured and predicted results. The results show that the Nord2000 method provides accurate calculations, while the ISO 9613-2 method can be used for simplified assessments of ILFN generated by wind turbines during the investment preparation phase.

Keywords: noise modelling; ISO 9613-2; CNOSSOS-EU; Nord2000; wind turbine noise; infrasonic and low-frequency noise; ILFN

check for updates

Citation: Stępień, B.; Wszołek, T.; Mleczko, D.; Małecki, P.; Pawlik, P.; Kłaczyński, M.; Czapla, M. Suitability Analysis of Selected Methods for Modelling Infrasound and Low-Frequency Noise from Wind Turbines. *Energies* **2024**, *17*, 2832. https://doi.org/10.3390/en17122832

Academic Editor: Francesco Castellani

Received: 17 February 2024
Revised: 4 June 2024
Accepted: 6 June 2024
Published: 8 June 2024

Copyright: © 2024 by the authors. Licensee MDPI, Basel, Switzerland. This article is an open access article distributed under the terms and conditions of the Creative Commons Attribution (CC BY) license (https://creativecommons.org/licenses/by/4.0/).

1. Introduction

Wind turbines are one of the most important sources of renewable energy [1]. They are widely promoted and used around the world to efficiently provide environmentally friendly energy [2]. One of the main disadvantages of wind turbines is the generation of infrasound and low-frequency noise (ILFN), which can cause annoyance and nuisance to nearby residents as well as people at a considerable distance from the turbine [3–5]. Therefore, the propagation of ILFN should be modelled at the stage of predicting the acoustic impact of wind turbines on the environment. Infrasound is defined as noise in the range of 1 Hz to 20 Hz [6,7], while low-frequency noise has no standardised definition. Different frequency range limits for this noise can be found in the literature. In the DIN 45680 standard [8], the low-frequency noise band is specified from 8 Hz to 100 Hz. According to Leventhall [9], low-frequency noise ranges from 10 Hz to 200 Hz, while according to ACGIH limits [10], infrasound and low-frequency noise is noise in the range of 1 Hz–80 Hz and according to other researchers up to 100 or 250 Hz or even 500 Hz [11–14]. In Poland, the Leventhall approach has been applied to low-frequency noise. In contrast, this study considers ILFN in octave bands with centre frequencies from 4 Hz to 250 Hz.

Many methods for modelling wind turbine noise can be found in the literature. The most common are complex methods that use different models. These include algorithms based on the "ray tracing" method [15–18], where the ray paths from each turbine source to each receiver are calculated based on favourable weather conditions or atmospheric inversion conditions. Current research is aimed at validating the models [16] and

extending the models to include multiple reflections from the ground and the influence of atmospheric turbulence [15].

ILFN can be modelled using a sequential approach that involves a Computational Fluid Dynamics (CFD) model, an aeroelastic HAWC model, and an acoustic model. This approach enables the analysis of how different factors and turbine design parameters affect the noise generated by turbines [19,20].

A theoretical method using Parabolic Equations (PE) [21–26], as well as the Fast Field Program (FFP) method [24], is also used to model ILFN generated by wind turbines.

Keith et al. [24] conducted a comparative analysis of sound pressure level (SPL) modelling results for infrasound and low-frequency sound. The results of calculations using the PE and FFP methods were compared with the results of calculations using the ISO 9613-2 method for the extended frequency range (below 63 Hz). These results were also compared with the results of long-term measurements carried out in Canada as part of the "Health Canada's Community Noise and Health Study" project.

Keith et al. [24], based on their study, clearly stated that sound speed profiles obtained from actual meteorological data can represent conditions not included in the Harmonoise weather classes. In such cases, SPL calculations using the Harmonoise class and actual meteorological conditions were similar at a distance of a few hundred metres from the turbine, while they differed by more than 20 dB at a distance of 10 km [24]. The authors also concluded that calculations using Harmonoise weather classes at long distances can lead to serious errors and recommend the use of actual meteorological profiles.

In conclusion, Keith et al. [24] state that the ISO 9613-2 extended the frequency calculation method can be used to calculate the annual average SPL of ILFN when the area to be assessed is within a few kilometres of the nearest wind turbines. When calculations need to be made for larger distances from the turbine or specific meteorological classes, the authors recommend using the FFP method using real atmospheric properties.

Bertagnolio et al. [27] investigated the possibility of using the coupling of the aeroelastic model HAWC2 and the so-called Formula 1A developed by Farassat to model the ILFN generated by a wind turbine operating upwind. The calculation results obtained with the above model were compared with other models used for modelling wind turbine noise, namely those of Viterna [28,29] and Amiet [30].

Bertagnolio et al. [27] analysed the influence of different factors and parameters on the level of the calculated ILFN at a point downstream of the turbine. The following were analysed: the influence of the time window of the Fourier analysis, the influence of the time step, the influence of the blade loading model, the influence of the tower and wind uplift, and the influence of the inflow turbulence and disturbance caused by the operation of the preceding turbine. The authors have shown that the proposed calculation method gives results that are consistent with other existing calculation methods. The main conclusion from these analyses is that the field disturbance caused by the preceding turbine has a significant effect on the estimate of the ILFN level generated by the turbine under study when the intensity of atmospheric turbulence is low. When the turbulence intensity is high, the influence of the field disturbance caused by the operation of the preceding turbine on the calculated ILFN level is low.

The computational model proposed in [27] has been verified experimentally in papers [31,32]. The authors compared the results of the numerical calculations with the measured results for two test wind turbines located at the DTU-Riso station. All meteorological input parameters to the model were determined from measured data recorded at the site. The authors found good agreement between the measured and calculated results when background noise is neglected. The results of the proposed model correctly reproduce the quantitative increase in the ILFN as a function of wind speed; although, in some cases, differences with the measured data are apparent in some frequency ranges [32].

However, research is still underway to improve methods for predicting wind turbine noise, as exemplified by the PIBE project [33], which was run in France from 2019 to 2023.

In papers [34,35], the authors have pointed out that the modelling of wind turbine noise requires the consideration of the wind turbine as an extended noise source together with aeroacoustic phenomena [36–38] as the main mechanisms for wind turbine noise generation. In contrast, the PIBE project showed that for distances up to 800 m in all propagation directions and for distances up to 1000 m for propagation directions from −120° to 120°, the effect of atmospheric turbulence on A-weighted sound pressure level predictions is negligible [39].

In a publication by Mascarenhas et al. [40], produced as part of the PIBE project, the authors presented the results of comparisons of wind turbine noise predictions (using a model combining Amiet's theory with a wide-angle parabolic equation) with field measurements. The results of the model and measurements were first compared at points close to the wind turbine and then at distances from 350 m to 1300 m from the source. Based on the results presented in this publication, the authors concluded that the model combining Amiet's theory with the wide-angle parabolic equation can be used for calculations in the frequency range from 100 Hz to 4 kHz. The authors also found that the turbulence dissipation rate parameter must be correctly estimated in order to accurately estimate the noise of a wind turbine at the receiving point for the model used. On the other hand, in publication [41], the authors presented a comparison of calculation results using a model combining Amiet's theory with a wide-angle parabolic equation with measured results in the 50 Hz to 10 kHz band for measurement points located upwind and downwind. The authors found that the model underestimated the measured results by about 2 dB for a measurement point at a distance of 1318 m from the nearest turbine in the frequency range below 200 Hz and above 400 Hz. This paper also shows that accurate prediction results can be obtained using this model for 1/3 octave band spectra averaged over 10 min for measurement points located up to 1300 m from a wind turbine.

All the above models are very complex and require specialised knowledge and the collection of input data that are very difficult or even impossible to obtain at the forecasting stage. These are mainly meteorological data that affect the generation of ILFN by the wind turbine (turbulence intensity, turbulence dissipation rate parameter) and its propagation (temperature gradient, wind speed gradient, wind direction in different parts of the atmosphere). For the above reasons, the engineering calculations commonly used in the prediction phase can be subject to very large uncertainties.

For the reasons outlined above, it is therefore necessary to use and improve existing computational methods (ISO 9613-2 [42], CNOSSOS-EU [43], and Nord2000 [44,45]) in engineering applications for modelling the ILFN generated by wind turbines.

Therefore, this paper identifies values for the differences between the calculated value (using three commonly used calculation methods) and the measured value of the sound pressure level generated by wind turbines in the 1/1 octave bands with centre frequencies from 4 Hz to 250 Hz. The sources of the differences are also identified to further work on these models to minimise these differences to a level acceptable for engineering applications.

2. Research Methods

2.1. Measurements of ILFN Generated by a Wind Turbine

An investigation was conducted to assess the usability and effectiveness of ISO 9613-2, CNOSSOS-EU, and Nord2000 algorithms in modelling the ILFN generated by wind turbines in octave frequency bands ranging from 4 Hz to 250 Hz. The study used real measurement data for three different average wind speeds measured at 10 m above ground level: 3.3 m/s, 4.2 m/s, and 4.6 m/s.

The noise source was a Vestas V90 wind turbine with a power output of 2 MW, located on a wind farm in central Poland (Figure 1). The hub of the turbine is installed at a height of 105 m, with a rotor diameter of 90 m.

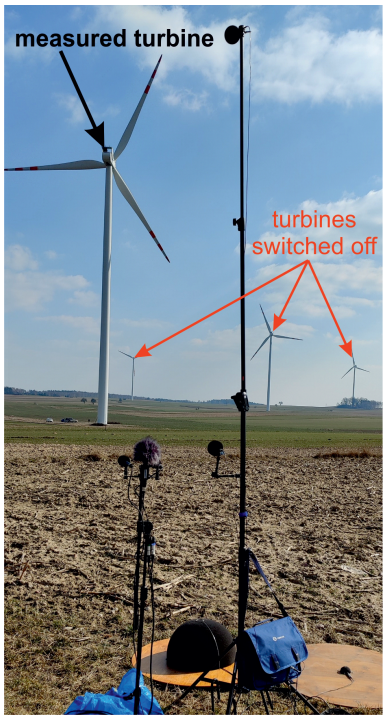

Figure 1. Vestas V90 turbine under investigation.

The sound power levels of the tested turbine were determined for each average wind speed analysed, following the guidelines of IEC 61400-11:2012/AMD1:2018 [46]. The recorded levels were 118.6 dB, 121.9 dB and 128.0 dB for wind speeds of 3.3 m/s, 4.2 m/s and 4.6 m/s, respectively. Figure 2 shows the sound power level spectra of the tested turbine in octave frequency bands.

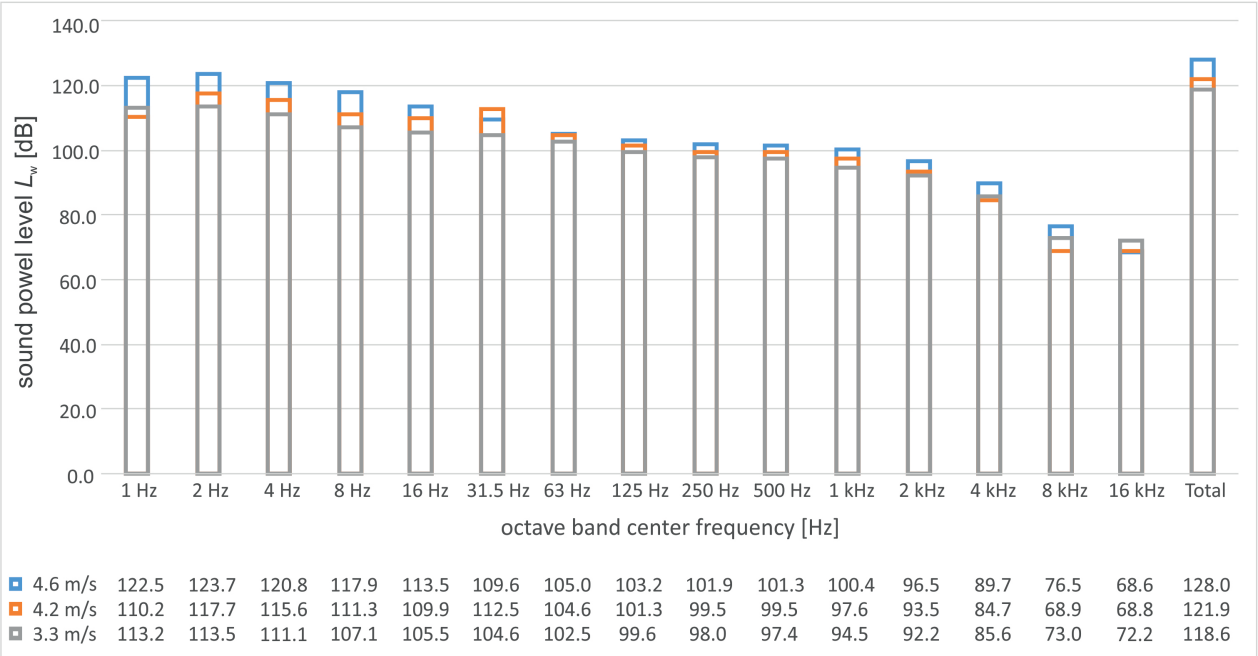

Figure 2. Sound power level spectrum of the tested Vestas V90 turbine for the analysed wind speeds.

Measurement points were located at distances of 250 m, 500 m, 1000 m and 1500 m behind the wind turbine (Figure 3) to test the utility of the ISO 9613-2, CNOSSOS-EU and Nord2000 computational algorithms for predicting the ILFN generated.

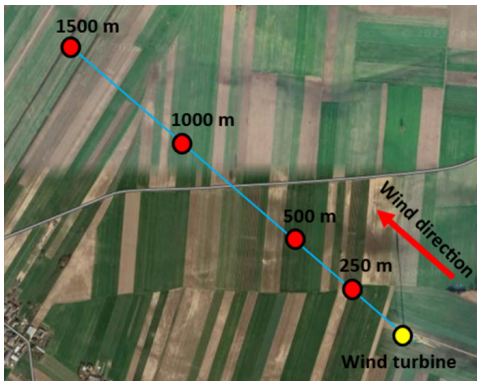

Figure 3. Location of measurement points. Source: google.maps.com.

Measurements were taken simultaneously at all measurement points to determine the sound power level and test the calculation algorithms. The measurement session lasted 24 h. Time intervals of 287 s for a wind speed of 3.3 m/s, 345 s for 4.2 m/s, and 731 s for 4.6 m/s were selected for analysis. The intervals were marked by consistent weather conditions, including wind speed and direction, temperature and humidity, and no other sound disturbances.

The sound level measurements were taken using multichannel sound level meters SVAN 958 (Svantek, Poland) equipped with ½″ G.R.A.S 40 AZ microphones with a frequency response of 0.5 Hz to 20 kHz and ½″ G.R.A.S 40 AE microphones with a frequency response of 3.15 Hz to 20 kHz. The measurements were taken at measurement points located at 0 m above ground level to minimize the influence of wind on the results [47]. The microphones were positioned on the measurement plates following the guidelines of IEC 61400-11:2012/AMD1:2018 [46].

Meteorological conditions during the measurements were recorded at various heights above ground level. Stations were placed at 10 m, 4 m and 1.5 m. Additionally, data from sensors located on the turbine hub, 105 m above ground level, were acquired. Calculations were based on the data recorded at 10 m. A summary of the recorded meteorological data is given in Table 1.

Table 1. Meteorological conditions recorded during measurements at different heights above ground level.

Location of the Meteorological Station above Ground Level	105 m	10 m	4 m	1.5 m
average wind speed: 3.3 m/s				
temperature [°C]	9.0	7.2	6.7	no data
static pressure [hPa]	no data	1013.7	no data	no data
relative humidity [%]	no data	46.3	59.0	no data
wind speed [m/s]	6.2	3.3	2.7	1.9
wind direction [°/description]	98.3–107.4	107.0–137.0	ESE	SE
average wind speed: 4.2 m/s				
temperature [°C]	9.0	6.2	5.7	no data
static pressure [hPa]	no data	1014.2	no data	no data
relative humidity [%]	no data	43.7	57.0	no data
wind speed [m/s]	8.0	4.2	3.3	2.2
wind direction [°/description]	107.7–109.6	126.0–148.0	SE	SE
average wind speed: 4.6 m/s				
temperature [°C]	9.0	6.2	5.6	no data
static pressure [hPa]	no data	1014.4	no data	no data
relative humidity [%]	no data	42.9	56.3	no data
wind speed [m/s]	8.0	4.6	3.7	2.7
wind direction [°/description]	107.7–109.6	119.0–148.0	SE-ESE	SE-ESE

2.2. Calculation Methods

Sections 2.2.1–2.2.3 present the sound propagation models analysed in this research. Each model is described briefly, without mathematical details.

2.2.1. ISO 9613-2

This model was introduced by the first edition of ISO 9613-2:1996 "Acoustics— Attenuation of sound during propagation outdoors—Part 2: General method of calculation" [48]. There is a lack of information on modelling methods for wind turbine noise. The first edition of ISO 9613-2 is recommended for use in Directive 2002/49/EC [49]. It is used for the prediction of sound pressure levels outdoors. The method can be applied to a variety of sound sources and covers the main sound attenuation mechanisms.

In 2024, the second edition of this standard was published as ISO 9613-2:2024 "Acoustics—Attenuation of sound during propagation outdoors—Part 2: Engineering method for the prediction of sound pressure levels outdoors" [42]. The second edition of ISO 9613-2 has been supplemented by issues related to the modelling of wind turbine noise, previously presented in "A good practice guide to the application of ETSU-R-97 for the assessment and rating of noise from wind farms" [50].

The model considers favourable sound propagation conditions in each direction from the source, assuming moderate temperature inversion above ground level and winds blowing at 1 m/s to 5 m/s at heights of 3 m to 11 m. It calculates long-term noise indices, A-weighted sound pressure level values and sound pressure level values in octave bands from 63 Hz to 8 kHz for sources located up to 30 m above ground level. The model considers sound absorption caused by differences in geometry between the source and receiver, as well as by the atmosphere, ground, barriers and sound wave reflections. The geometry and characteristics of the ground are crucial for the calculations made using this model.

The accuracy of the method is ±3 dB for distances between 100 m and 1000 m and source heights up to 30 m. However, the accuracy of the method is not specified for distances greater than 1 km [51]. It is recommended to add 3 dB to the sound pressure level results when the receiver is located in a valley [52].

The sound pressure level at the receiving point is calculated for each frequency band using the following equation [42]:

$$L_{ft}(\mathrm{DW}) = L_{\mathrm{W}} + D_{\mathrm{c}} - A \qquad [\mathrm{dB}], \tag{1}$$

where

$L_{ft}(\mathrm{DW})$ is the equivalent sound pressure level at the receiver point for the octave band;
L_{W} is the sound power level of the source for the octave band;
D_{c} is the directivity correction; for an omnidirectional source, $D_{\mathrm{c}} = 0$;
A is the attenuation of the sound propagation determined from the following equation [42]:

$$A = A_{\mathrm{div}} + A_{\mathrm{atm}} + A_{\mathrm{gr}} + A_{\mathrm{bar}} + A_{\mathrm{misc}} \qquad [\mathrm{dB}], \tag{2}$$

where

A_{div} is the attenuation due to geometrical divergence;
A_{atm} is the attenuation due to atmospheric absorption;
A_{gr} is the attenuation due to the ground effect;
A_{bar} is the attenuation due to a barrier;
A_{misc} is the attenuation due to miscellaneous other effect.

When performing calculations using the ISO 9613-2 model, it is also necessary to know the geometric parameters of the turbine (hub height and rotor diameter). It is also necessary to know the meteorological conditions at the site of the wind turbine (relative humidity, air pressure, temperature, wind speed and direction). This model uses the algorithm described in the ISO 9613-1 [53] standard to calculate the sound absorption by the atmosphere.

2.2.2. CNOSSOS-EU

The CNOSSOS-EU model was introduced and detailed in the European Commission Directive 2015/996 [43] and supplemented in 2020 by Commission Delegated Directive (EU) 2021/1226 [54]. This model replaced the algorithms recommended in Directive 2002/49/EC [49] to harmonise the calculation methods used in the countries of the European Union, thus making it possible to directly compare the acoustic climate prevailing in the different Member States.

The model is used to calculate outdoor sound pressure levels for any type of environment (rural environment, urban environment, U-shaped roads) and can be applied to different types of sound sources, taking into account the main sound attenuation mechanisms along the propagation path. The model does not apply to the calculation of propagation over water (lake, wide river, etc.) [55].

With this model, it is possible to perform calculations for two types of weather conditions [43]:

- Favourable propagation conditions (F)—sound propagation with downward refraction of sound rays (positive vertical gradient of the effective sound propagation speed) from the source to the receiver;
- Homogeneous propagation conditions (H)—sound propagation with no downward refraction of sound rays (zero vertical gradient of the speed of sound propagation) over the entire propagation area.

The CNOSSOS-EU model allows the calculation of long-term noise indicators, A-weighted sound level values and sound pressure level values in octave bands from 63 Hz to 8 kHz for receivers located at least 2 m above ground level at a distance of up to 800 m from the source. The calculation of long-term indicators is based on the sum of the sound levels for homogeneous (L_H) and favourable (L_F) conditions, weighted by the percentage of favourable propagation conditions p.

The sound pressure level is calculated for each frequency band using the following equation [43]:

$$L_{F/H} = L_W - A_{F/H} \quad [dB], \tag{3}$$

where
$L_{F/H}$ is the equivalent sound pressure level at the receiver point in the octave band for favourable (F) and homogeneous (H) propagation conditions;
L_W is the sound power level of the source for the octave band;
$A_{F/H}$ is the total attenuation determined from Equation [43]:

$$A_{F/H} = A_{div\ F/H} + A_{atm\ F/H} + A_{boundary\ F/H} \quad [dB], \tag{4}$$

where
$A_{div\ F/H}$ is the attenuation due to geometrical divergence;
$A_{atm\ F/H}$ is the attenuation due to atmospheric absorption;
$A_{boundary\ F/H}$ is the attenuation due to the boundary of the propagation medium determined from Equation [43]:

$$A_{boundary\ F/H} = A_{ground\ F/H} + A_{dif\ F/H} \quad [dB], \tag{5}$$

where
$A_{ground\ F/H}$ is the attenuation due to the ground;
$A_{dif\ F/H}$ is the attenuation due to diffraction.

When performing calculations using the CNOSSOS-EU model, it is also necessary to know the geometric parameters of the turbine (hub height and rotor diameter). It is also necessary to know the meteorological conditions at the site of the wind turbine (relative humidity, air pressure, temperature, wind speed and direction, percentage of favourable propagation conditions). This model uses the algorithm described in the ISO 9613-1 [53] standard to calculate the sound absorption by the atmosphere.

2.2.3. Nord2000

The Nord2000 model has been developed by the Nordic countries (Denmark, Finland, Norway and Sweden) to predict the propagation of environmental noise over water and land surfaces. The model uses the radial method and the diffraction theory [56]. The model can be used to calculate equivalent sound pressure levels, total A-weighted sound pressure levels and sound pressure levels in one-third octave frequency bands from 25 Hz to 10 kHz [57]. The model can be used for calculations in hilly terrain as it takes into account differences in terrain topography [58] and conditions with and without refraction of sound rays [51].

The model can be used to calculate short-term and long-term noise indicators for homogeneous and heterogeneous weather conditions. The calculation of long-term indicators is based on the determination of short-term indicators taking into account the statistical parameters of the meteorological conditions. The accuracy of the model is ±2 dB [44].

The Nord2000 model takes into account the actual meteorological conditions at the time of measurement. The temperature and wind profile have a significant influence on the sound speed profile. The temperature profile disturbs the wind profile and consequently the sound speed profile. The sound rays are deflected downwards or upwards depending on the wind and temperature profile. The roughness length is used in the model to define the wind speed profile [58]. The classification of roughness length varies according to the type of land cover [59].

The sound pressure level at the receiving point is calculated for each frequency band using the following equation [58]:

$$SPL = L_W + \Delta L_d + \Delta L_a + \Delta L_t + \Delta L_s + \Delta L_r \quad [dB], \tag{6}$$

where

SPL is the sound pressure level at the receiver point for the frequency band;
L_W is the sound power level of the source for the frequency band;
ΔL_d is the propagation effect of spherical divergence;
ΔL_a is the propagation effect of the atmospheric absorption;
ΔL_t is the propagation effect of the terrain;
ΔL_s is the propagation effect of the scattering zones;
ΔL_r is the propagation effect of obstacles.

When performing calculations using the Nord2000 model, it is also necessary to know the geometric parameters of the turbine (hub height and rotor diameter). It is also necessary to know the meteorological conditions at the site of the wind turbine (roughness length, relative humidity, air pressure, temperature, temperature gradient, standard deviation of temperature gradient, structure parameter of turbulent temperature fluctuations, wind speed and direction, standard deviation of wind speed, structure parameter of turbulent wind speed fluctuations) and anemometer height. This model uses the algorithm described in the ISO 9613-1 [53] standard to calculate the sound absorption by the atmosphere.

2.3. Statistical Methods

2.3.1. Kruskal–Wallis Test

The Kruskal–Wallis [60] test is one of the most popular non-parametric alternatives to one-way analysis of variance (ANOVA), and an extension of the Wilcoxon–Mann–Whitney test to more than two samples [61]. The Kruskal–Wallis test is used when the assumptions of ANOVA are not met, or when the nature of the variables does not allow the use of ANOVA [62].

The null hypothesis of the Kruskal–Wallis test assumes that the compared samples are from the same population or, equivalently, from different populations with the same distribution at the assumed level of significance α. This test compares the medians of the samples being compared. The Kruskal–Wallis test uses the χ^2 statistic to test the hypothesis.

The χ^2 statistic replaces the F-statistic used in classical one-way ANOVA. Ranks are the basis for the calculation of statistics in this test, not numerical values.

The significant result of the Kruskal–Wallis test indicates that there are statistically significant differences between the samples at the chosen level of significance. To check between which samples these differences occur, a multiple comparison test should be performed.

2.3.2. Tukey–Kramer Test

The result of the Kruskal–Wallis (Section 2.3.1) test indicates that there are differences between the samples being compared. A post hoc analysis should be performed to determine which samples have statistically significant differences. This involves performing a multiple comparison test. One such test is the Tukey–Kramer test. This test was developed by Tukey [63] in 1949 for samples of the same size and extended by Kramer [64] in 1956 for samples of different sizes. For this reason, it is often referred to in the literature as the Tukey–Kramer test [65].

The null hypothesis for the Tukey–Kramer test is that all the means that are being compared are from the same population. The test statistic q_s of this test is compared with the critical value q_α for the assumed significance level α from the table for the studentized range distribution [63,64]. The means differ significantly at the α level if the value q_s is greater than the critical value q_α obtained from the distribution.

The Tukey–Kramer test also allows the calculation of confidence intervals for the compared means. The comparison of these confidence intervals in the figure provides a graphical presentation of the results of the multiple comparisons performed for the compared samples. The means of two samples are statistically different at the assumed significance level α if their intervals are disjoint, but they are not significantly different if their intervals overlap [66].

2.3.3. Spearman's Rank Correlation Coefficient

Spearman's correlation is an analysis that allows variables on an ordinal and quantitative scale that do not have a normal distribution to be correlated with each other. This is a type of non-parametric correlation based on ranks. It is recommended for use when there are outliers in the samples being analysed. It is very insensitive to them because it examines the correlation between ranks, not the values of the variables [67].

The Spearman correlation coefficient (r_S) is the Pearson correlation coefficient calculated for the ranks of the variables [68]. It is used to test for any monotonic relationship between data. The Spearman correlation coefficient is more general than the Pearson correlation coefficient, which only measures a linear relationship.

The value of the (r_S) coefficient is in the closed interval $[-1, 1]$. When analysing the correlation, there are two factors to consider:

1. The strength of the correlation:
   - For $|r_S| < 0.2$, there is no correlation;
   - For $|r_S| \in < 0.2, 0.4)$, there is a weak correlation;
   - For $|r_S| \in < 0.4, 0.7)$, there is a moderate correlation;
   - For $|r_S| \in < 0.7, 0.9 >$, there is a strong correlation;
   - For $|r_S| > 0.9$, there is a very strong correlation.
2. The direction of the correlation (the type of relationship):
   - If $r_S > 0$, there is a positive correlation (this means that the variables are positively correlated);
   - If $r_S < 0$, there is a negative correlation (this means that the variables are negatively correlated).

3. Research Results

3.1. Results of Measurements

Upon analysing the data presented in Table 1, it is evident that a temperature inversion phenomenon occurred during the measurements, whereby the air temperature increased with height above ground level. Additionally, there was an increase in wind speed with height and a slight shift in wind direction.

Table 2 displays the sound pressure levels in octave frequency bands measured at various distances behind the operating turbine ($L_{90,250}$, $L_{90,500}$, $L_{90,1000}$, $L_{90,1500}$), along with the corresponding background sound levels ($L_{B90,250}$, $L_{B90,500}$, $L_{B90,1000}$, $L_{B90,1500}$) recorded at the same measurement points when all the wind turbines on the farm were switched off. The sound pressure level generated by the operating turbine and the background sound level were estimated using the L_{90} statistical level. The time segments of the recorded signals selected for analysis corresponded to stable meteorological conditions. The results shown in Table 2 are also presented graphically in Figure 4.

Table 2. Sound pressure levels recorded at the measurement points.

Distance	Indicator	Octave Band Center Frequency						
[m]	[dB]	4 Hz	8 Hz	16 Hz	31.5 Hz	63 Hz	125 Hz	250 Hz
average wind speed: 3.3 m/s								
250	$L_{90,250}$	53.8	50.9	50.3	49.5	47.6	45.3	42.6
	$L_{B90,250}$	54.0	51.1	50.4	42.3	40.7	32.8	27.6
500	$L_{90,500}$	51.2	48.7	46.8	45.4	**43.3**	38.2	35.2
	$L_{B90,500}$	53.5	49.0	47.1	42.3	**40.7**	32.8	27.6
1000	$L_{90,1000}$	55.3	49.8	47.6	**48.3**	**43.9**	38.3	32.5
	$L_{B90,1000}$	55.4	50.1	48.4	**45.5**	**41.7**	34.3	28.1
1500	$L_{90,1500}$	**49.1**	**45.1**	**44.8**	**46.1**	**43.6**	**33.6**	**26.8**
	$L_{90,1500}$	**48.0**	**44.3**	**44.3**	**44.0**	**42.6**	**33.4**	**25.9**
average wind speed: 4.2 m/s								
250	$L_{90,250}$	58.8	55.9	54.9	54.7	50.5	47.8	45.9
	$L_{B90,250}$	53.5	49.0	47.1	42.3	40.7	32.8	27.6
500	$L_{90,500}$	56.5	53.4	51.5	48.7	44.2	40.3	38.2
	$L_{B90,500}$	53.5	49.0	47.1	42.3	40.7	32.8	27.6
1000	$L_{90,1000}$	**56.5**	**52.4**	**49.8**	**46.4**	**44.3**	39.1	33.7
	$L_{B90,1000}$	**55.4**	**50.1**	**48.4**	**45.5**	**41.7**	34.3	28.1
1500	$L_{90,1500}$	53.8	49.1	**46.7**	**44.0**	**43.6**	**34.5**	**28.2**
	$L_{90,1500}$	48.0	44.3	**44.3**	**42.7**	**42.6**	**33.4**	**25.9**
average wind speed: 4.6 m/s								
250	$L_{90,250}$	59.4	56.2	55.0	52.7	51.0	49.0	47.4
	$L_{B90,250}$	53.5	49.0	47.1	42.3	40.7	32.8	27.6
500	$L_{90,500}$	**55.2**	**51.7**	50.9	47.2	44.6	42.0	40.6
	$L_{B90,500}$	**53.5**	**49.0**	47.1	42.3	40.7	32.8	27.6
1000	$L_{90,1000}$	55.2	**51.1**	**49.7**	**46.5**	45.6	40.2	35.7
	$L_{B90,1000}$	55.4	**50.1**	**48.4**	**45.5**	41.7	34.3	28.1
1500	$L_{90,1500}$	**50.5**	**46.1**	**45.8**	**43.7**	**44.1**	**34.8**	29.8
	$L_{90,1500}$	**48.0**	**44.3**	**44.3**	**42.7**	**42.6**	**33.4**	25.9

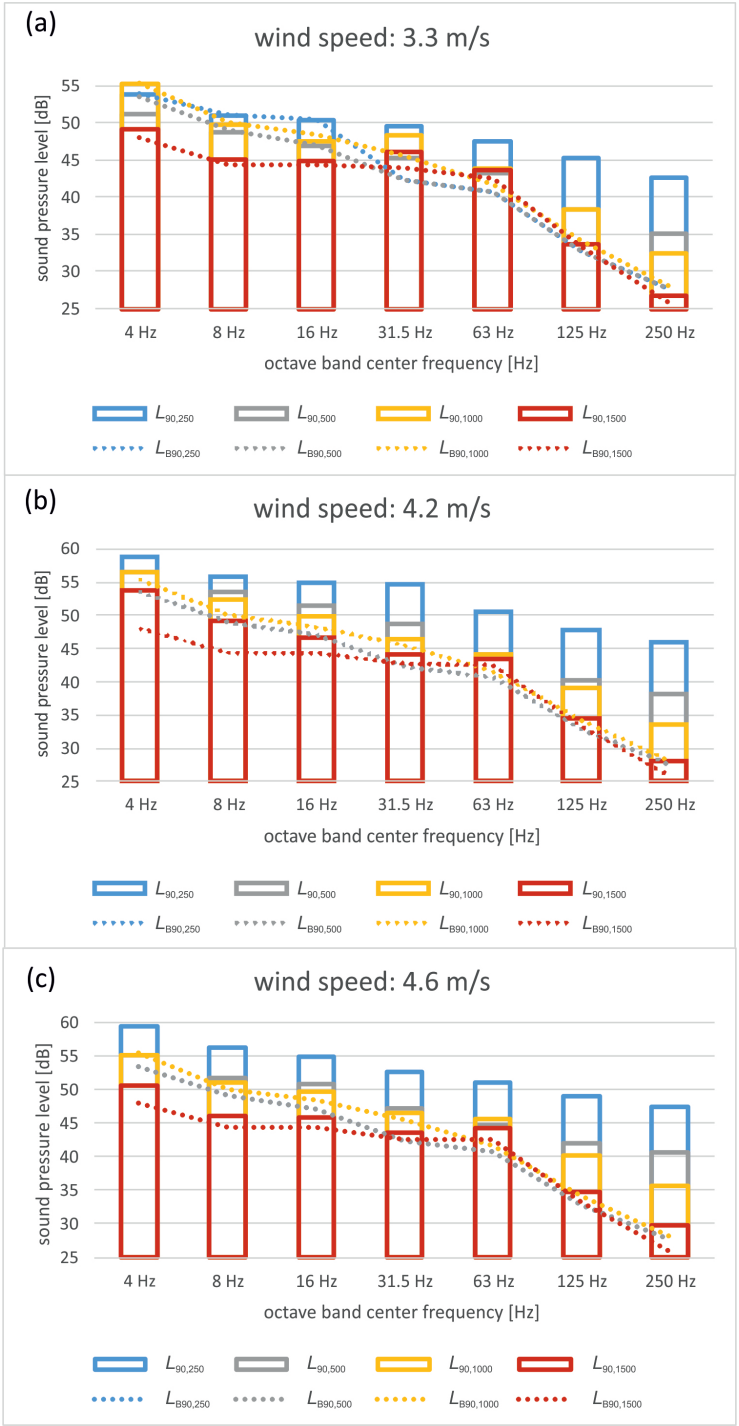

Figure 4. The spectrum of the sound pressure level generated by the operating turbine and the background sound pressure level at the analysed points for the following: (**a**) An average wind speed of 3.3 m/s. (**b**) An average wind speed of 4.2 m/s. (**c**) An average wind speed of 4.6 m/s. $L_{90,250}$—sound pressure level during turbine operation at a distance of 250 m behind the turbine; $L_{B90,250}$—background sound pressure level at a distance of 250 m behind the turbine; $L_{90,500}$—sound pressure level during turbine operation at a distance of 250 m behind the turbine; $L_{B90,500}$—background sound pressure level at a distance of 250 m behind the turbine; $L_{90,1000}$—sound pressure level during turbine operation at a distance of 250 m behind the turbine; $L_{B90,1000}$—background sound pressure level at a distance of 250 m behind the turbine; $L_{90,1500}$—sound pressure level during turbine operation at a distance of 250 m behind the turbine; $L_{B90,1500}$—background sound pressure level at a distance of 250 m behind the turbine.

For ten octave bands, a higher background sound pressure level was recorded than the sound pressure level recorded during the turbine operation. Such cases were recorded for the bands of 4 Hz, 8 Hz and 16 Hz at a measurement points 250 m, 500 m and 1000 m behind the turbine for an average wind speed of 3.3 m/s, and for the band 4 Hz at measurement point 1000 m from the turbine for an average wind speed of 4.6 m/s. These bands are highlighted in grey in Table 2. These differences range from 0.1 dB to 2.3 dB (4 Hz, 500 m).

In Table 2, marked in bold are the frequency bands where the difference between the sound pressure level recorded during turbine operation and the background sound pressure level is less than 3 dB. This fact makes it impossible to measure the noise emissions of wind turbines. A total of 31 such bands were recorded, including 10 for an average wind speed of 3.3 m/s, 10 for an average wind speed of 4.2 m/s and 11 for an average wind speed of 4.6 m/s.

3.2. Results of Calculations

In order to test the suitability of the computational algorithms presented in Section 2.2 for the modelling of ILFN generated by wind turbines, a model of the wind farm and calculations were performed in SoundPlan software ver. 8.2 , meeting the requirements of the ISO 17534 series of standards [69–72], which is commonly used for modelling sound level distribution in the environment [73].

A wind turbine has been modelled as a source of noise with a sound power level determined from measurements (see Section 2.1). Based on the elevation and land use maps and the documentation collected during the site visit, a numerical model was developed.

The following assumptions were made in order to build the numerical model:

- The model takes into account the digital ground model;
- The model reproduced the actual ground cover around the turbine and included all relevant elements affecting the calculation of sound propagation in the environment (buildings fixed to the ground, woodland, rivers, lakes);
- All elements have a real height.

In the final stage of building a model for all types, screening, attenuation and noise sources, integration of non-acoustic data with acoustic data was carried out. This resulted in a complete acoustic model of the wind farm from which ILFN levels were calculated in octave frequency bands ranging from 4 Hz to 250 Hz at selected calculation points corresponding to the measurement points.

Calculations were performed using three commonly used computational models: ISO 9613-2, CNOSSOS-EU for favourable propagation conditions, and Nord2000, taking into account the weather conditions prevailing during the measurement session, which was recorded at an altitude of 10 m above ground level (Table 1). Calculations and analyses were carried out for octave frequency bands with centre frequencies ranging from 4 Hz to 250 Hz. The results of the sound pressure level measurements obtained for all three average wind speeds analysed were then compared with the calculation results obtained using the ISO 9613-2 algorithm (Tables 3, A5 and A9), CNOSSOS-EU (Tables 4, A1 and A11) and Nord2000 (Tables 5, A3 and A7). These tables show the background-corrected measured sound pressure level generated by the operating turbine $L_{p,m}$, the calculated sound pressure level using the analysed calculation algorithms $L_{p,c}$ and the differences between these parameters $\Delta L_p = L_{p,c} - L_{p,m}$.

Tables 6–8, A2, A4, A6, A8, A10 and A12 show the minimum and maximum absolute values of the difference between the calculated and measured sound pressure level $\left(\Delta L_{p,abs}\right)$.

This chapter contains only selected tables comparing the measured results with the predicted results of the sound pressure level generated by the operating wind turbine (Tables 3–5) and selected statistical parameters of the $\Delta L_{p,abs}$ value (Tables 6–8). Other tables can be found in the Appendix B.

Table 3. Comparison of measurement and calculation results obtained using the ISO 9613-2 model for measurement points located at different distances behind the turbine for an average wind speed of 3.3 m/s.

Distance	Indicator	Octave Band Center Frequency						
[m]	[dB]	4 Hz	8 Hz	16 Hz	31.5 Hz	63 Hz	125 Hz	250 Hz
250	$L_{p,m}$	—	—	—	48.5	46.6	45.0	42.4
	$L_{p,c}$	49.8	45.9	44.6	44.2	44.0	42.8	41.0
	ΔL_p	—	—	—	−4.3	−2.6	−2.2	−1.4
500	$L_{p,m}$	—	—	—	42.4	39.8	36.8	34.3
	$L_{p,c}$	49.0	44.9	43.4	42.4	40.3	37.2	35.4
	ΔL_p	—	—	—	0.0	0.5	0.4	1.1
1000	$L_{p,m}$	—	—	—	45.0	39.9	36.1	30.6
	$L_{p,c}$	38.3	34.3	32.8	31.9	29.9	27.2	26.3
	ΔL_p	—	—	—	−13.1	−10.0	−8.9	−4.3
1500	$L_{p,m}$	42.5	37.3	35.2	41.8	36.5	21.1	19.7
	$L_{p,c}$	34.8	30.8	29.2	28.4	26.3	23.4	22.0
	ΔL_p	−7.7	−6.5	−6.0	−13.5	−10.2	2.3	2.3

Table 4. Comparison of measurement and calculation results obtained using the CNOSSOS-EU model for measurement points located at different distances behind the turbine for an average wind speed of 4.2 m/s.

Distance	Indicator	Octave Band Center Frequency						
[m]	[dB]	4 Hz	8 Hz	16 Hz	31.5 Hz	63 Hz	125 Hz	250 Hz
250	$L_{p,m}$	57.4	54.8	54.1	54.4	50.1	47.6	45.9
	$L_{p,c}$	55.9	51.6	50.2	52.8	44.8	41.5	39.5
	ΔL_p	−1.5	−3.2	−3.9	−1.6	−5.3	−6.1	−6.4
500	$L_{p,m}$	53.4	51.5	49.6	47.5	41.6	39.5	37.8
	$L_{p,c}$	50.5	46.1	44.7	47.4	39.4	36.0	33.9
	ΔL_p	−2.9	−5.4	−4.9	−0.1	−2.2	−3.5	−3.9
1000	$L_{p,m}$	50.1	48.4	42.2	39.2	40.7	37.3	32.3
	$L_{p,c}$	44.5	40.2	38.8	41.4	33.4	29.8	27.4
	ΔL_p	−5.6	−8.2	−5.4	2.2	−7.3	−7.5	−4.9
1500	$L_{p,m}$	52.5	47.3	42.9	38.3	36.5	28.0	24.3
	$L_{p,c}$	41.0	36.7	35.3	37.9	29.8	26.1	23.5
	ΔL_p	−11.5	−10.6	−7.6	−0.4	−6.7	−1.9	−0.8

Table 5. Comparison of measurement and calculation results obtained using the Nord2000 model for measurement points located at different distances behind the turbine for an average wind speed of 4.6 m/s.

Distance	Indicator	Octave Band Center Frequency						
[m]	[dB]	4 Hz	8 Hz	16 Hz	31.5 Hz	63 Hz	125 Hz	250 Hz
250	$L_{p,m}$	58.1	55.2	54.2	52.2	50.6	48.8	47.4
	$L_{p,c}$	67.0	64.2	59.7	55.7	50.8	48.7	46.8
	ΔL_p	8.9	9.0	5.5	3.5	0.2	−0.1	−0.6

Table 5. *Cont.*

Distance	Indicator	Octave Band Center Frequency						
[m]	[dB]	4 Hz	8 Hz	16 Hz	31.5 Hz	63 Hz	125 Hz	250 Hz
500	$L_{p,m}$	50.3	48.4	48.6	45.6	42.4	41.4	40.4
	$L_{p,c}$	61.6	58.7	54.2	49.9	44.4	42.1	39.8
	ΔL_p	11.3	10.3	5.6	4.3	2.0	0.7	−0.6
1000	$L_{p,m}$	—	44.2	43.9	39.6	43.3	39.0	34.9
	$L_{p,c}$	55.7	52.7	48.1	43.8	38.3	34.4	30.8
	ΔL_p	—	8.5	4.2	4.2	−5.0	−4.6	−4.1
1500	$L_{p,m}$	46.9	41.4	40.5	36.8	38.9	29.3	27.6
	$L_{p,c}$	52.2	49.2	44.5	40.0	34.0	30.4	26.4
	ΔL_p	5.3	7.8	4.0	3.2	−4.9	1.1	−1.2

Table 6. Selected statistical parameters of the absolute values of the differences between measured and calculated values using the ISO 9613-2 model for an average wind speed of 3.3 m/s.

Parameters	Distance from the Turbine			
[dB]	250 m	500 m	1000 m	1500 m
min	1.4	0.0	4.3	2.3
max	4.3	1.1	13.1	13.5

Table 7. Selected statistical parameters of the absolute values of the differences between measured and calculated values using the CNOSSOS-EU model for an average wind speed of 4.2 m/s.

Parameters	Distance from the Turbine			
[dB]	250 m	500 m	1000 m	1500 m
min	1.5	0.1	2.2	0.4
max	6.4	5.4	8.2	11.5

Table 8. Selected statistical parameters of the absolute values of the differences between measured and calculated values using the Nord2000 model for an average wind speed of 4.6 m/s.

Parameters	Distance from the Turbine			
[dB]	250 m	500 m	1000 m	1500 m
min	0.1	0.6	4.1	1.1
max	9.0	11.3	8.5	7.8

4. Analysis of Results

The absolute values of the differences between the calculated and measured value $\left(\Delta L_{p,abs}\right)$ using the ISO 9613-2 method of the sound pressure level generated by the wind turbine for an average wind speed of 3.3 m/s (Table 6) range from 0.0 dB (31.5 Hz, 500 m) to 13.5 dB (31.5 Hz, 1500 m). For the average wind speed of 4.2 m/s, they range from 0.1 dB to 13.2 dB for the 4 Hz band at 500 m and 1500 m, respectively. In contrast, for the highest average wind speed analysed, 4.6 m/s, the absolute values of $\Delta L_{p,abs}$ range from 0.2 dB (8 Hz, 1500 m) to 10.9 dB (63 Hz, 1000 m).

At the measurement points 250 m, 500 m and 1000 m from the turbine for octave bands with centre frequencies of 4 Hz, 8 Hz, 16 Hz (Tables 3, A1 and A3), and for the band 4 Hz at a measurement point 1000 m from the turbine (Tables 5, A9 and A11), the difference between the calculated and measured value of the sound pressure level was not determined. This is because the ILFN emission level generated by the wind turbine was not determined at these measurement points for the aforementioned frequency bands because the recorded

value of the background sound pressure level was higher than the sound pressure level recorded during turbine operation.

The measurement and calculation results obtained for each calculation method at all measurement points for an average wind speed of 3.3 m/s are shown in Figure A1, while the values of the differences ΔL_p between the calculated value $L_{p,c}$ and the measured value $L_{p,m}$ are shown in Figure 5. In the ideal case of agreement between the model results and the measured values, each curve representing a given model should be flat and its value should be 0 dB. It can be seen that the ΔL_p values for each method at a given measurement point form parallel lines. Only for the 250 m point does the line of difference obtained for the ISO 9613-2 method cross the line for the CNOSSOS-EU method, and for the 63 Hz–250 Hz frequency bands, the ΔL_p values for the ISO 9613-2 method are smaller than for the CNOSSOS-EU method. For a measurement point 500 m away, the ΔL_p values for the ISO 9613-2 and Nord2000 methods from the 31.5 Hz frequency band approach each other and for the 250 Hz band are very similar. For measurement points 1000 m and 1500 m away, the lines move closer together as the frequency of the band analysed increases, and in the 250 Hz band, the ΔL_p values for each method are very similar.

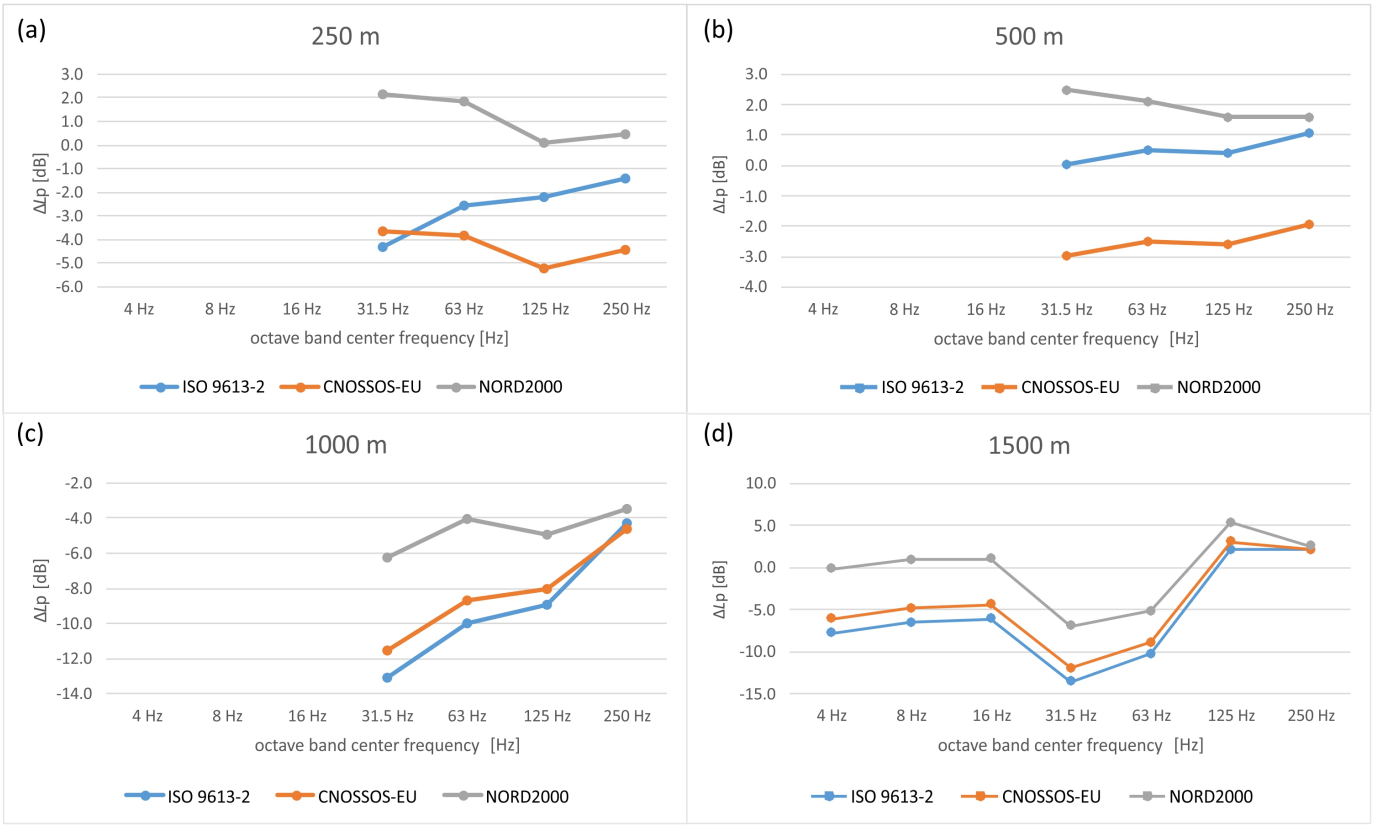

Figure 5. Differences between calculated and measured values (ΔL_p) of the sound pressure level generated by a wind turbine for an average wind speed of 3.3 m/s: (**a**) At a distance 250 m. (**b**) At a distance 500 m. (**c**) At a distance 1000 m. (**d**) At a distance 1500 m.

The $\Delta L_{p,abs}$ values determined for the prediction results using the CNOSSOS-EU algorithm for favourable propagation conditions at an average wind speed of 3.3 m/s range from 1.9 dB (250 Hz, 500 m) to 11.9 dB (31.5 Hz, 1500 m). For an average wind speed of 4.2 m/s (Table 7), they range from 0.1 dB to 11.5 dB for the 31.5 Hz band at 500 m and the 4 Hz band at 1500 m, respectively. In contrast, for an average wind speed of 4.6 m/s, the absolute values of ΔL_p range from 0.2 dB (16 Hz, 500 m) to 9.6 dB (63 Hz, 1000 m).

The ΔL_p difference values obtained at a given measurement point for each calculation method at an average wind speed of 4.2 m/s are shown in Figure 6, while the results of the measurement and calculation are shown in Figure A2. As in the case of an average

wind speed of 3.3 m/s, the curves ΔL_p are parallel and, for a measurement point 250 m away, the line of difference values obtained for the ISO 9613-2 method intersects the line for the CNOSSOS-EU method. As a result, the ΔL_p values for the ISO 9613-2 method are smaller than those for the CNOSSOS-EU method in the 63 Hz, 125 Hz and 250 Hz frequency bands. For a measurement point at a distance of 500 m, the ΔL_p values for the ISO 9613-2 and Nord2000 methods from the 31.5 Hz frequency band approach each other and for the 250 Hz band are almost identical. On the other hand, at 1000 m and 1500 m, the lines move closer together as the frequency of the band analysed increases, and at 250 Hz, the ΔL_p values for each method are very similar.

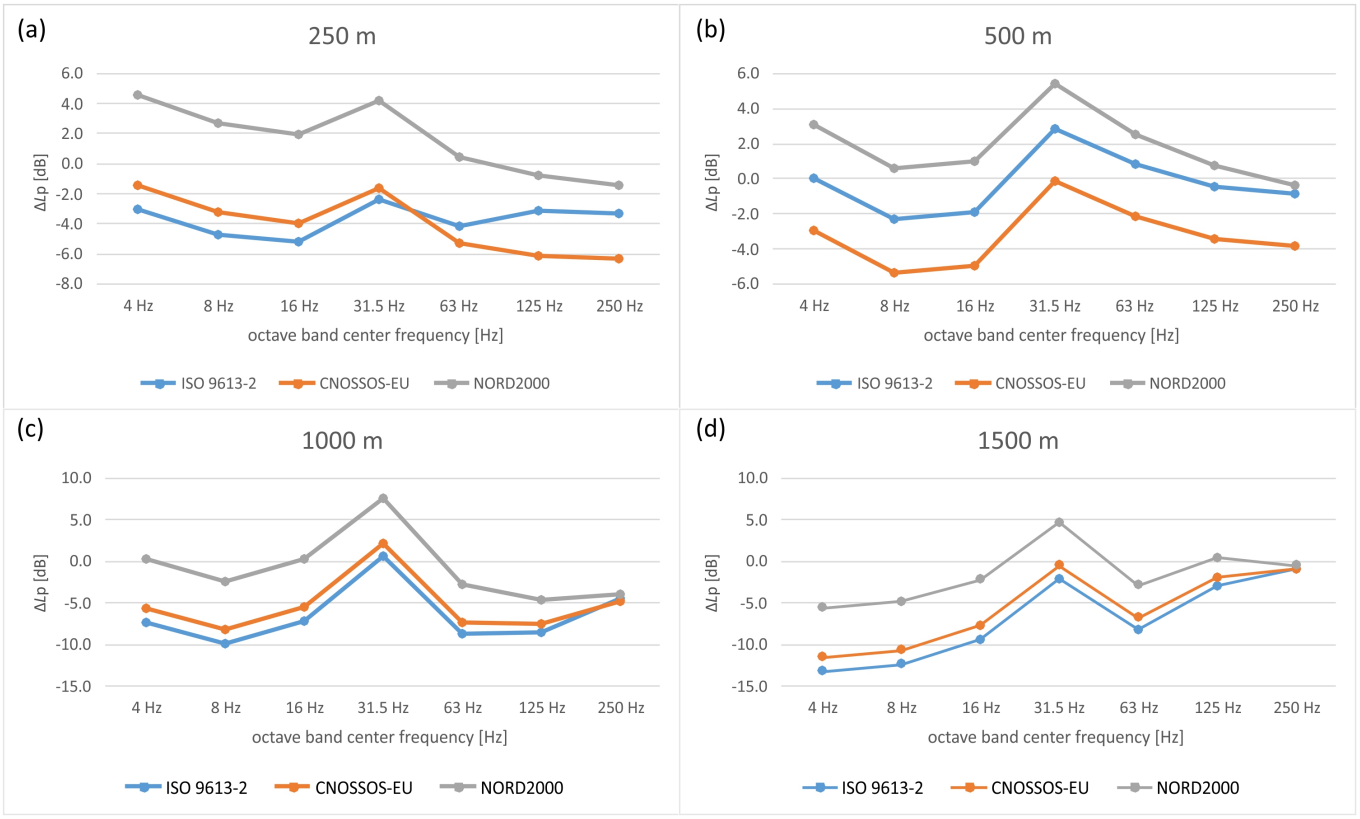

Figure 6. Differences between calculated and measured values (ΔL_p) of the sound pressure level generated by a wind turbine for an average wind speed of 4.2 m/s: (**a**) At a distance 250 m. (**b**) At a distance 500 m. (**c**) At a distance 1000 m. (**d**) At a distance 1500 m.

The absolute values of the differences between the calculated and measured values $\left(\Delta L_{p,abs}\right)$ using the Nord2000 method of the sound pressure level generated by an operating wind turbine for an average wind speed of 3.3 m/s range from 0.0 dB (4 Hz, 1500 m) to 6.9 dB (31.5 Hz, 1500 m). At an average wind speed of 4.2 m/s, they range from 0.3 dB to 7.6 dB at the measurement point at a distance of 1000 m, for the 16 Hz and 31.5 Hz frequency bands, respectively. On the other hand, for an average wind speed of 4.6 m/s, the absolute values of $\Delta L_{p,abs}$ (Table 8) range from 0.1 dB (125 Hz, 250 m) to 11.3 dB (4 Hz, 500 m).

The values of the differences ΔL_p between the calculated value of $L_{p,c}$ and the measured value of $L_{p,m}$ obtained at measurement points at distances of 250 m, 500 m, 1000 m and 1500 m for each calculation method at an average wind speed of 4.6 m/s are shown in Figure 7, while Figure A3 shows the measured and calculated results for the same points. As with the two previous average wind speeds analysed, the curves ΔL_p shown in Figure 7 are parallel up to a frequency band of 63 Hz and then begin to converge as the frequency increases. Only at a point 250 m from the turbine does the ΔL_p curve obtained for the ISO 9613-2 method cross the curve for the CNOSSOS-EU method. The ΔL_p values obtained

for the CNOSSOS-EU method in the frequency bands 63 Hz–250 Hz are higher than those obtained for the ISO 9613-2 method. For the 500 m measurement point, the ΔL_p values for the ISO 9613-2 and Nord2000 methods in the 250 Hz band are almost identical, while for the 1000 m and 1500 m points, the ΔL_p values for the 250 Hz frequency band are very similar for all three calculation methods analysed.

Non-parametric statistical tests were performed to check for statistically significant differences between the measured results $(L_{p,m})$ and the predicted results $(L_{p,c})$ obtained for the calculation methods used. These tests were carried out on 12 sets of data: all the measurement points (4 points) and all the average wind speeds analysed (3 average wind speeds) for the whole frequency range analysed.

First, the Kruskal–Wallis test (Section 2.3.1) was performed at a significance level of $\alpha = 0.05$. The results of this test clearly showed that there were no statistically significant differences between the measurement results and the prediction results at the significance level chosen. The obtained test probability values ranged from 0.08 to 0.60. However, a non-parametric Tukey–Kramer multiple comparison test (Section 2.3.2) was also performed to determine which of the calculation methods used produced results most similar to the measurement results. Analysis of the results of the Tukey–Kramer test showed that in eight cases the results obtained using the Nord2000 method were closest to the measurement results. The results obtained using the ISO 9613-2 method were closest to the measured results in three cases (250 m, 4.6 m/s; 500 m, 3.3 m/s and 4.2 m/s) and for the CNOSSOS-EU method in one case (500 m, 4.6 m/s).

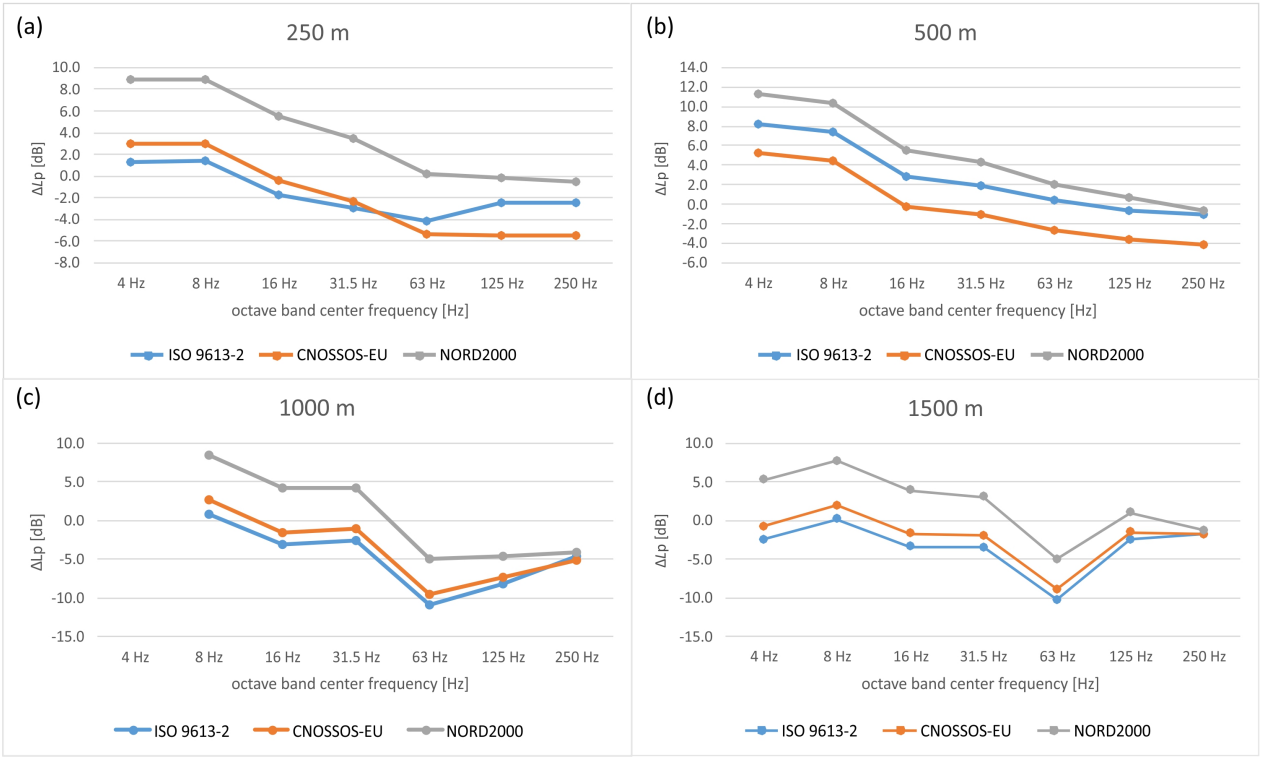

Figure 7. Differences between calculated and measured values (ΔL_p) of the sound pressure level generated by a wind turbine for an average wind speed of 4.6 m/s: (**a**) At a distance 250 m. (**b**) At a distance 500 m. (**c**) At a distance 1000 m. (**d**) At a distance 1500 m.

The same test procedure was performed for the value of the differences (ΔL_p) between the calculated and measured results. In this case, it was found that statistically significant differences for $\alpha = 0.05$ occurred in 8 of the 12 data sets analysed (marked in bold in Table 9). In the remaining four cases, there were no statistically significant differences. The test probability values obtained from the Kruskal–Wallis test performed on the ΔL_p differences are shown in Table 9.

Table 9. Probability values (p-values) of the Kruskal–Wallis test carried out for differences ΔL_p.

Average Wind Speed	Distance from the Turbine			
	250 m	**500 m**	**1000 m**	**1500 m**
3.3 m/s	**0.003**	**0.02**	**0.01**	0.26
4.2 m/s	$\mathbf{1.25 \cdot 10^{-4}}$	$\mathbf{7.59 \cdot 10^{-4}}$	**0.01**	**0.002**
4.6 m/s	0.05	0.05	0.12	**0.01**

A non-parametric test for multiple comparisons was also performed at a significance level of $\alpha = 0.05$ to determine for which method the differences in ΔL_p were closest to zero (the ideal case of agreement between the model results and the measured values). The results of this test are very similar to those of the previous test procedure performed for predicted and measured results. The ΔL_p differences closest to zero were obtained using the Nord2000 calculation method in the nine data sets analysed. The ISO 9613-2 method had difference results closest to zero in two data sets (500 m, 3.3 m/s; 500 m, 4.2 m/s), while CNOSSOS-EU had only one (500 m, 4.6 m/s).

Analysing the results of the tests carried out, it can be concluded that the ISO 9613-2 method performs best for distances up to 500 m from the turbine for all the average wind speeds analysed, while in other cases, the Nord2000 method gives much more accurate results.

Analysing the measured $(L_{p,m})$ and calculated $(L_{p,c})$ sound pressure levels shown in Figures A1–A3, it can be seen that the shape of the octave spectrum is well reproduced by all three calculation methods analysed for all cases.

In order to confirm this objectively, a correlation analysis was carried out between the measured and calculated ILFN values generated by the wind turbine for all cases analysed. For this purpose, the Spearman correlation coefficient (r_S) was determined, as the acoustic data do not have a normal distribution [74].

The values of the correlation coefficient (r_S) are shown in Table 10 and they range from 0.79 to 1.00. This means that there is a strong and very strong positive correlation between the measurement and calculation results. Based on the values of the Spearman correlation coefficient, it is clear that all the computational models analysed reproduce the shape of the ILFN octave spectrum very well in all the cases analysed.

The values of the correlation coefficients determined between measured and calculated values have the same value for each calculation method in almost all cases analysed. Only at a distance of 250 m from the turbine, for an average wind speed of 4.6 m/s, the value of the correlation coefficient between measured and calculated values for the ISO 9613-2 method is slightly lower than for the other two methods.

The suspicions arising from the analysis of Figures A1–A3 were objectively confirmed by the correlation analysis carried out between the measured and calculated results.

Table 10. The Spearman correlation coefficients (r_S) between measured $(L_{p,m})$ and calculated $(L_{p,c})$ values.

Distance	250 m	500 m	1000 m	1500 m
average wind speed: 3.3 m/s				
(measurement, ISO 9613-2)	1.00	1.00	1.00	0.82
(measurement, CNOSSOS-EU)	1.00	1.00	1.00	0.82
(measurement, Nord2000)	1.00	1.00	1.00	0.82
average wind speed: 4.2 m/s				
(measurement, ISO 9613-2)	0.96	0.89	0.79	0.89
(measurement, CNOSSOS-EU)	0.96	0.89	0.79	0.89
(measurement, Nord2000)	0.96	0.89	0.79	0.89

Table 10. *Cont.*

Distance	250 m	500 m	1000 m	1500 m
average wind speed: 4.6 m/s				
(measurement, ISO 9613-2)	0.99	0.96	0.94	0.96
(measurement, CNOSSOS-EU)	1.00	0.96	0.94	0.96
(measurement, Nord2000)	1.00	0.96	0.94	0.96

5. Summary and Conclusions

In this paper, a measurement verification of the prediction results of the ILFN generated by a wind turbine obtained by the ISO 9613-2, CNOSSOS-EU and Nord2000 methods has been carried out. The aim was to test the suitability of these models for the determination of sound pressure levels in octave frequency bands in the range from 4 Hz to 250 Hz.

For this purpose, a geometric-acoustic model of a wind farm operating in central Poland was created in the SoundPlan software. The SoundPlan software was also used to calculate the sound pressure levels using the above calculation methods.

The prediction results were compared with the actual measurements taken at the wind farm in question. Calculations and measurements were carried out for points located at distances of 250 m, 500 m, 1000 m and 1500 m behind the turbine at 0 m above ground level. The calculation points and the measurement microphones were placed on a measuring plate according to the guidelines of IEC 61400-11:2012/AMD1:2018 [46] with a single windscreen. The analysis was carried out for octave bands with centre frequencies from 4 Hz to 250 Hz for three average wind speeds (3.3 m/s, 4.2 m/s and 4.6 m/s) recorded at 10 m above ground level.

The absolute values of the differences between calculated and measured results for the ISO 9613-2 method range from 0.0 dB (3.3 m/s, 500 m, 31.5 Hz) to 13.5 dB (3.3 m/s, 1500 m, 31. 5 Hz), for the CNOSSOS-EU method from 0.1 dB (4.2 m/s, 500 m, 31.5 Hz) to 11.9 dB (3.3 m/s, 1500 m, 31.5 Hz) and the Nord2000 method from 0.0 dB (3.3 m/s, 1500 m, 4 Hz) to 11.3 dB (4.6 m/s, 500 m, 4 Hz).

The differences ΔL_p shown in Figures 5–7 obtained for each method form parallel lines over the whole frequency band analysed, regardless of the average wind speed used in the calculations. Overall, it can be concluded that the Nord2000 model overestimates the results by an average of 0.8 dB, while the ISO 9613-2 and CNOSSOS-EU models underestimate the results by an average of 3.4 dB and 3.8 dB, respectively.

It was also noted that the prediction results obtained using the ISO 9613-2 method are 3 dB higher than those obtained using the CNOSSOS-EU method for each octave frequency band analysed between 4 Hz and 250 Hz, but only at the calculation point 500 m downstream of the turbine regardless of wind speed.

The differences between calculated and measured values depend on several factors. The most important are the following:

- A different height of the source location above ground level (105 m) than assumed in the calculation methods (according to the ISO 9613-2 and CNOSSOS-EU calculation methods, the maximum height of the source location should not exceed a value of 30 m);
- A different value of the ground coefficient G used in the calculations than in reality, due to the angle of incidence of the sound wave on the ground;
- The difference between the actual values of the sound absorption coefficients of the ground and the atmosphere and the values assumed for the calculations;
- In the ISO 9613-2 and CNOSSOS-EU models, it is not possible to take into account the direction and speed of the wind;
- It is not possible to take into account the wind speed and direction for the different atmospheric layers present in the propagation path of an acoustic wave.

Non-parametric statistical tests were performed at a significance level of $\alpha = 0.05$ to determine whether there were statistically significant differences between the predicted

and measured results of the ILFN generated by the wind turbines. A total of 12 data sets were analysed. The calculation results obtained for the Nord2000 method were closest to the measurements in eight cases, for the ISO 9613-2 method in three cases and for the CNOSSOS-EU method in only one case.

The same test procedure was also applied to the value of the differences (ΔL_p) between the calculated and measured results. Once again, 12 sets of data were analysed. In nine cases the (ΔL_p) differences were closest to zero for the Nord2000 method, in two cases for the ISO 9613-2 method and only one case for the CNOSSOS-EU method.

As a result of the tests, it was found that the most accurate results were obtained using the Nord2000 calculation method, and the least accurate results were obtained using the CNOSSOS-EU model.

A correlation analysis was also carried out between the results of the calculations $(L_{p,c})$ for each method and the results of the measurements $(L_{p,m})$. The Spearman's rank correlation coefficients were determined for this purpose. All models showed a strong or very strong correlation with the measurement results, which means that they represent the shape of the spectrum in the analysed frequency range very well.

It is not easy to verify the calculation results obtained using the ISO 9613-2 and CNOSSOS-EU models in specific wind conditions by measurement. This is because these models do not take into account the wind speed and direction recorded during the measurements. The ISO 9613-2 method assumes that there are favourable propagation conditions in all directions from the source to the receiver. The CNOSSOS-EU method, on the other hand, allows calculations to be made for homogeneous or favourable sound propagation conditions, assuming that the same propagation conditions prevail in all directions from the source to the receiver. Favourable propagation conditions in all directions do not exist in reality. Homogeneous conditions are sometimes encountered.

Such limitations are not present in the assumptions of the Nord2000 method. The model allows the calculation of sound pressure levels under specific meteorological conditions. To perform such calculations, knowledge of wind direction and speed, air pressure, relative humidity and air temperature is required, as well as knowledge of parameters such as roughness length, temperature gradient, standard deviation of temperature gradient, structure parameter of turbulent temperature fluctuations, standard deviation of wind speed and structure parameter of turbulent wind speed fluctuations.

Taking into account all the analyses carried out, as well as the amount and availability of data input to the model for predicting ILFN generated by wind turbines, it was concluded that the Nord2000 model can be used for calculations with increased accuracy (on average, the results are overestimated by 0.8 dB), but with high labour intensity. This model requires input data that are difficult to obtain. These are mainly the meteorological data mentioned in the previous paragraph.

On the other hand, in the case of the ISO 9613-2 model, the collection of the required input data is not problematic, but the accuracy of the prediction results is lower than in the case of the Nord2000 model. The results obtained using the ISO 9613-2 model are underestimated by an average of 3.4 dB. This model can therefore be used for simplified calculations with lower accuracy.

In order to obtain accurate ILFN modelling results, it is necessary to build an accurate digital twin of the wind farm to be analysed, taking into account all important elements that affect the attenuation of sound during propagation outdoors (landform, land cover, land use). All parameters required by a given calculation method (turbine sound power level, turbine geometric dimensions, turbine operating schedule, meteorological conditions prevailing in a given area) should be determined with the highest precision available. A very important element influencing the accuracy of the calculations is the determination of the sound attenuation coefficient by the atmosphere for each frequency band analysed. For this purpose, its value should be determined based on Equations (3)–(5) given in the ISO 9613-1.

The research results presented in this article relate only to the measurement verification of ILFN calculations generated by a working wind turbine under specific meteorological

conditions for three average wind speeds. The research results and analyses presented indicate that these computational models can be successfully used to predict ILFN from wind turbines. Therefore, it seems reasonable to carry out a measurement verification of the ILFN prediction results obtained with the ISO 9613-2, CNOSSOS-EU and Nord2000 methods for a longer period (e.g., one year), taking into account the different sound propagation conditions. This research may help to identify a model that should be used to determine long-term noise hazard indicators (L_{DEN}, L_N), as well as indicators describing the harmful effects of noise, which include Ischaemic Heart Disease (IHD), High Annoyance (HA) and High Sleep Disturbance (HSD), in accordance with Commission Directive (EU) 2020/367 [75].

Author Contributions: Conceptualization, B.S., T.W., P.P. and P.M.; methodology, B.S., T.W. and P.P.; software, B.S.; validation, B.S., T.W., D.M., P.M., P.P. and M.K.; formal analysis, B.S.; investigation, B.S., D.M. and P.M.; resources, B.S., D.M., P.M. and M.C.; data curation, B.S., D.M. and P.M.; writing—original draft preparation, B.S. and T.W.; writing—review and editing, B.S., T.W., P.M., P.P., M.K. and M.C.; visualization, B.S. and M.C.; supervision, T.W.; project administration, T.W.; funding acquisition, T.W. All authors have read and agreed to the published version of the manuscript.

Funding: The research leading to these results has received funding from the Norway Grants 2014–2021 through the National Centre for Research and Development (project No. NOR/POLNOR/Hetman/0073/2019-00) and by the Polish Ministry of Science and Higher Education—project No. 16.16.130.942.

Data Availability Statement: The original contributions presented in the study are included in the article, further inquiries can be directed to the corresponding author.

Conflicts of Interest: The authors declare no conflicts of interest.

Appendix A

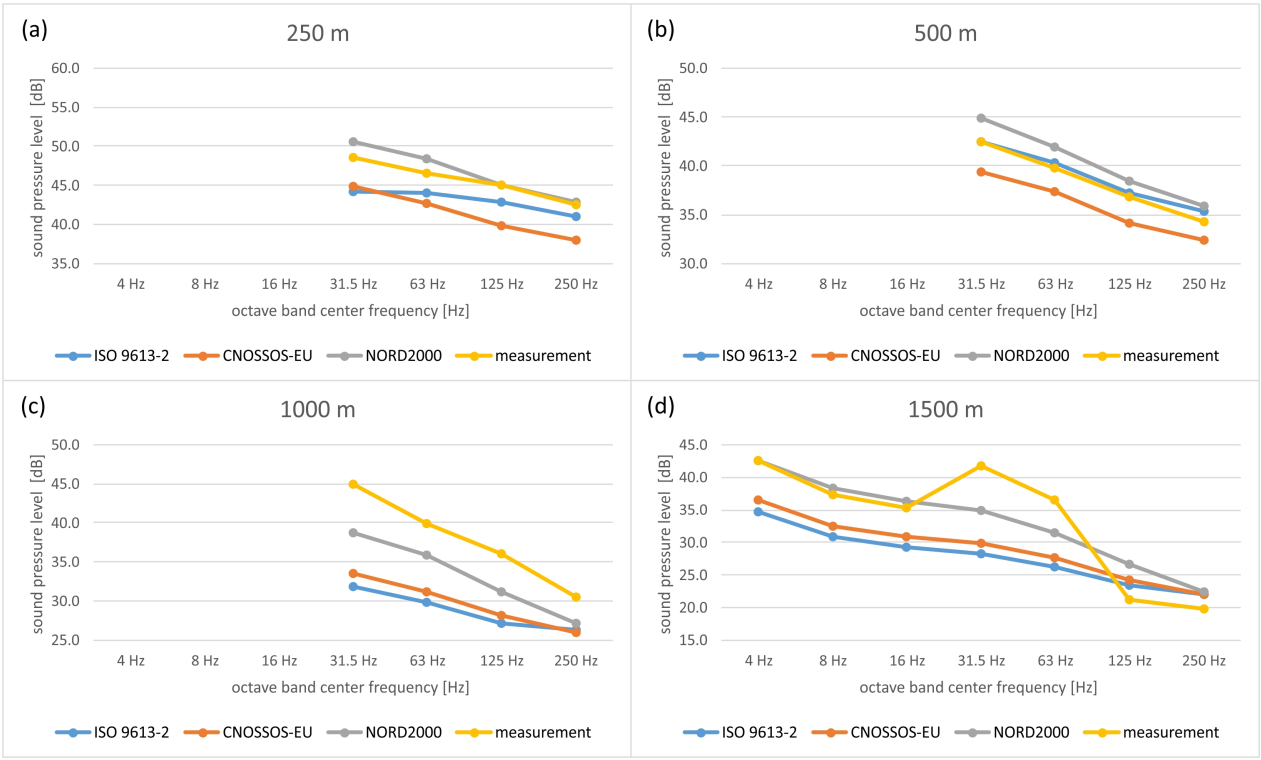

Figure A1. Calculated and measured values of the sound pressure level generated by a wind turbine for an average wind speed of 3.3 m/s: (**a**) At a distance 250 m. (**b**) At a distance 500 m. (**c**) At a distance 1000 m. (**d**) At a distance 1500 m.

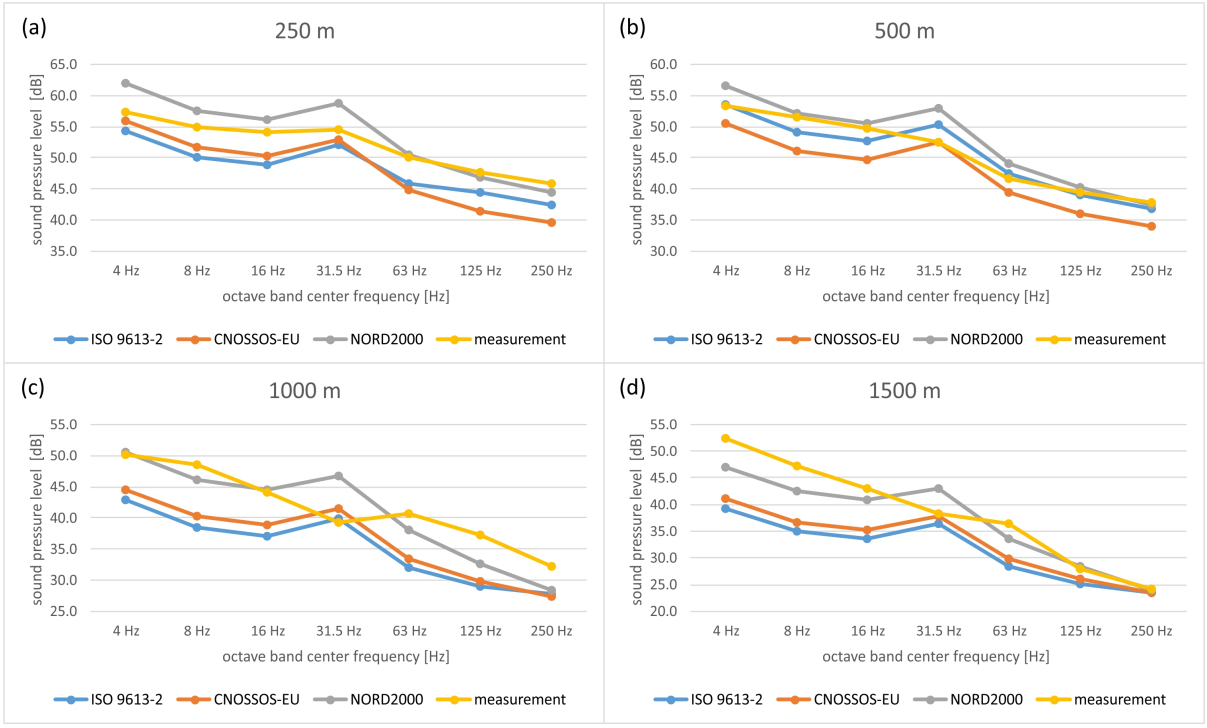

Figure A2. Calculated and measured values of the sound pressure level generated by a wind turbine for an average wind speed of 4.2 m/s: (**a**) At a distance 250 m. (**b**) At a distance 500 m. (**c**) At a distance 1000 m. (**d**) At a distance 1500 m.

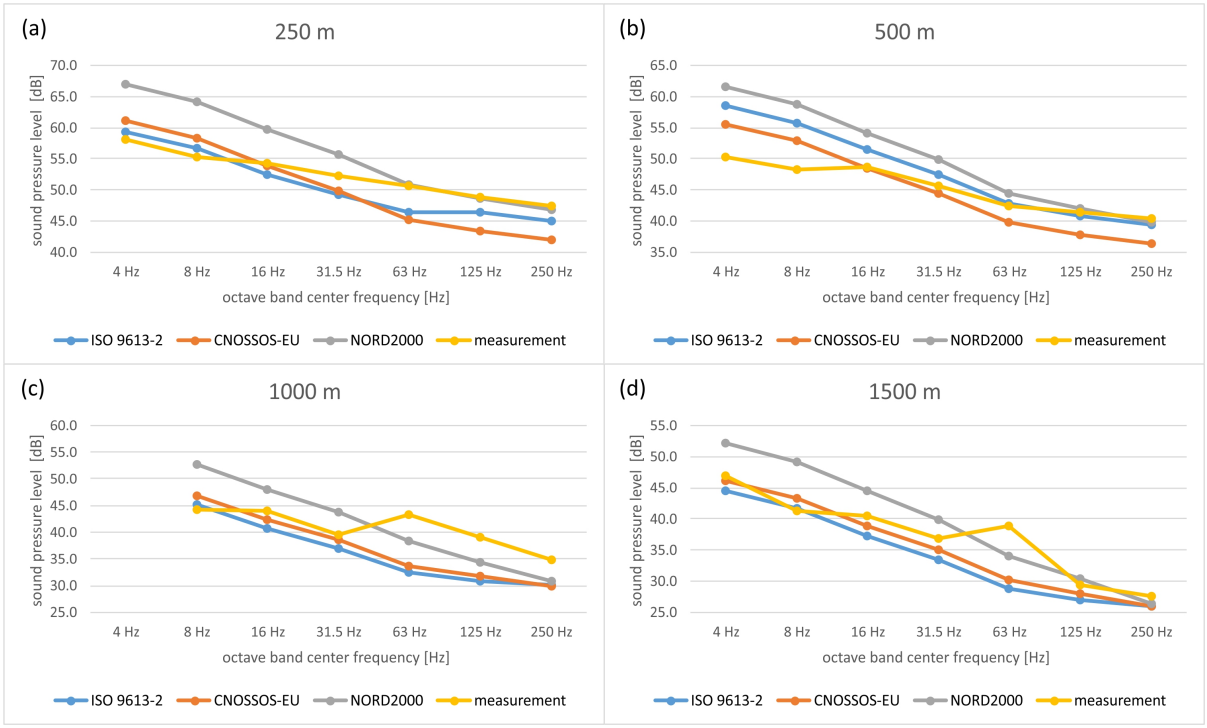

Figure A3. Calculated and measured values of the sound pressure level generated by a wind turbine for an average wind speed of 4.6 m/s: (**a**) At a distance 250 m. (**b**) At a distance 500 m. (**c**) At a distance 1000 m. (**d**) At a distance 1500 m.

Appendix B

Appendix B.1. Results for an Average Wind Speed of 3.3 m/s

Table A1. Comparison of measurement and calculation results obtained using the CNOSSOS-EU model for measurement points located at different distances behind the turbine for an average wind speed of 3.3 m/s.

Distance	Indicator	Octave Band Center Frequency						
[m]	[dB]	4 Hz	8 Hz	16 Hz	31.5 Hz	63 Hz	125 Hz	250 Hz
250	$L_{p,m}$	—	—	—	48.5	46.6	45.0	42.4
	$L_{p,c}$	51.4	47.4	45.8	44.9	42.7	39.8	38.0
	ΔL_p	—	—	—	−3.7	−3.9	−5.2	−4.4
500	$L_{p,m}$	—	—	—	42.4	39.8	36.8	34.3
	$L_{p,c}$	46.0	41.9	40.4	39.4	37.3	34.2	32.4
	ΔL_p	—	—	—	−3.0	−2.5	−2.6	−1.9
1000	$L_{p,m}$	—	—	—	45.0	39.9	36.1	30.6
	$L_{p,c}$	40.0	36.0	34.4	33.5	31.2	28.1	26.0
	ΔL_p	—	—	—	−11.6	−8.7	−8.0	−4.6
1500	$L_{p,m}$	42.5	37.3	35.2	41.8	36.5	21.1	19.7
	$L_{p,c}$	36.5	32.5	30.9	30.0	27.7	24.3	22.0
	ΔL_p	−6.0	−4.8	−4.3	−11.9	−8.8	3.2	2.3

Table A2. Selected statistical parameters of the absolute values of the differences between measured and calculated values using the CNOSSOS-EU model for an average wind speed of 3.3 m/s.

Parameters	Distance from the Turbine			
[dB]	250 m	500 m	1000 m	1500 m
min	3.7	1.9	4.6	2.3
max	5.2	3.0	11.6	11.9

Table A3. Comparison of measurement and calculation results obtained using the Nord2000 model for measurement points located at different distances behind the turbine for an average wind speed of 3.3 m/s.

Distance	Indicator	Octave Band Center Frequency						
[m]	[dB]	4 Hz	8 Hz	16 Hz	31.5 Hz	63 Hz	125 Hz	250 Hz
250	$L_{p,m}$	—	—	—	48.5	46.6	45.0	42.4
	$L_{p,c}$	57.4	53.3	51.7	50.7	48.4	45.1	42.9
	ΔL_p	—	—	—	2.1	1.8	0.1	0.5
500	$L_{p,m}$	—	—	—	42.4	39.8	36.8	34.3
	$L_{p,c}$	52.0	47.9	46.2	44.9	41.9	38.4	35.9
	ΔL_p	—	—	—	2.5	2.1	1.6	1.6
1000	$L_{p,m}$	—	—	—	45.0	39.9	36.1	30.6
	$L_{p,c}$	46.0	41.9	40.1	38.8	35.9	31.2	27.1
	ΔL_p	—	—	—	−6.3	−4.0	−4.9	−3.5
1500	$L_{p,m}$	42.5	37.3	35.2	41.8	36.5	21.1	19.7
	$L_{p,c}$	42.5	38.3	36.4	35.0	31.4	26.6	22.4
	ΔL_p	0.0	1.0	1.2	−6.9	−5.1	5.5	2.7

Table A4. Selected statistical parameters of the absolute values of the differences between measured and calculated values using the Nord2000 model for an average wind speed of 3.3 m/s.

Parameters [dB]	Distance from the Turbine 250 m	500 m	1000 m	1500 m
min	0.1	1.6	3.5	0.0
max	2.1	2.5	6.3	6.9

Appendix B.2. Results for an Average Wind Speed of 4.2 m/s

Table A5. Comparison of measurement and calculation results obtained using the ISO 9613-2 model for measurement points located at different distances behind the turbine for an average wind speed of 4.2 m/s.

Distance [m]	Indicator [dB]	Octave Band Center Frequency 4 Hz	8 Hz	16 Hz	31.5 Hz	63 Hz	125 Hz	250 Hz
250	$L_{p,m}$	57.4	54.8	54.1	54.4	50.1	47.6	45.9
	$L_{p,c}$	54.3	50.1	48.9	52.0	45.9	44.5	42.5
	ΔL_p	−3.1	−4.7	−5.2	−2.4	−4.2	−3.1	−3.4
500	$L_{p,m}$	53.4	51.5	49.6	47.5	41.6	39.5	37.8
	$L_{p,c}$	53.5	49.2	47.7	50.4	42.4	39.0	36.9
	ΔL_p	0.1	−2.3	−1.9	2.9	0.8	−0.5	−0.9
1000	$L_{p,m}$	50.1	48.4	44.2	39.2	40.7	37.3	32.3
	$L_{p,c}$	42.8	38.5	37.1	39.9	32.0	28.9	27.8
	ΔL_p	−7.3	−9.9	−7.1	0.7	−8.7	−8.4	−4.5
1500	$L_{p,m}$	52.5	47.3	42.9	38.3	36.5	28.0	24.3
	$L_{p,c}$	39.3	35.0	33.6	36.3	28.4	25.1	23.5
	ΔL_p	−13.2	−12.3	−9.3	−2.0	−8.1	−2.9	−0.8

Table A6. Selected statistical parameters of the absolute values of the differences between measured and calculated values using the ISO 9613-2 model for an average wind speed of 4.2 m/s.

Parameters [dB]	Distance from the Turbine 250 m	500 m	1000 m	1500 m
min	2.4	0.1	0.7	0.8
max	5.2	2.9	9.9	13.2

Table A7. Comparison of measurement and calculation results obtained using the Nord2000 model for measurement points located at different distances behind the turbine for an average wind speed of 4.2 m/s.

Distance [m]	Indicator [dB]	Octave Band Center Frequency 4 Hz	8 Hz	16 Hz	31.5 Hz	63 Hz	125 Hz	250 Hz
250	$L_{p,m}$	57.4	54.8	54.1	54.4	50.1	47.6	45.9
	$L_{p,c}$	61.9	57.5	56.1	58.7	50.5	46.9	44.4
	ΔL_p	4.5	2.7	2.0	4.2	0.4	−0.7	−1.5
500	$L_{p,m}$	53.4	51.5	49.6	47.5	41.6	39.5	37.8
	$L_{p,c}$	56.5	52.1	50.6	52.9	44.1	40.2	37.4
	ΔL_p	3.1	0.6	1.0	5.4	2.5	0.7	−0.4

Table A7. *Cont.*

Distance	Indicator	Octave Band Center Frequency						
[m]	[dB]	4 Hz	8 Hz	16 Hz	31.5 Hz	63 Hz	125 Hz	250 Hz
1000	$L_{p,m}$	50.1	48.4	44.2	39.2	40.7	37.3	32.3
	$L_{p,c}$	50.5	46.1	44.5	46.8	38.0	32.7	28.4
	ΔL_p	0.4	−2.3	0.3	7.6	−2.7	−4.6	−3.9
1500	$L_{p,m}$	52.5	47.3	42.9	38.3	36.5	28.0	24.3
	$L_{p,c}$	47.0	42.6	40.8	43.1	33.7	28.5	23.9
	ΔL_p	−5.5	−4.7	−2.1	4.8	−2.8	0.5	−0.4

Table A8. Selected statistical parameters of the absolute values of the differences between measured and calculated values using the Nord2000 model for an average wind speed of 4.2 m/s.

Parameters	Distance from the Turbine			
[dB]	250 m	500 m	1000 m	1500 m
min	0.4	0.4	0.3	0.4
max	4.5	5.4	7.6	5.5

Appendix B.3. Results for an Average Wind Speed of 4.6 m/s

Table A9. Comparison of measurement and calculation results obtained using the ISO 9613-2 model for measurement points located at different distances behind the turbine for an average wind speed of 4.6 m/s.

Distance	Indicator	Octave Band Center Frequency						
[m]	[dB]	4 Hz	8 Hz	16 Hz	31.5 Hz	63 Hz	125 Hz	250 Hz
250	$L_{p,m}$	58.1	55.2	54.2	52.2	50.6	48.8	47.4
	$L_{p,c}$	59.4	56.7	52.5	49.3	46.4	46.4	44.9
	ΔL_p	1.3	1.5	−1.7	−3.0	−4.2	−2.4	−2.5
500	$L_{p,m}$	50.3	48.4	48.6	45.6	42.4	41.4	40.4
	$L_{p,c}$	58.6	55.8	51.4	47.5	42.8	40.8	39.3
	ΔL_p	8.3	7.4	2.8	1.9	0.4	−0.6	−1.1
1000	$L_{p,m}$	—	44.2	43.9	39.6	43.3	39.0	34.9
	$L_{p,c}$	48.0	45.1	40.8	37.0	32.4	30.8	30.2
	ΔL_p	—	0.9	−3.1	−2.7	−10.9	−8.2	−4.7
1500	$L_{p,m}$	46.9	41.4	40.5	36.8	38.9	29.3	27.6
	$L_{p,c}$	44.5	41.6	37.2	33.4	28.7	26.9	25.9
	ΔL_p	−2.4	0.2	−3.3	−3.4	−10.2	−2.4	−1.7

Table A10. Selected statistical parameters of the absolute values of the differences between measured and calculated values using the ISO 9613-2 model for an average wind speed of 4.6 m/s.

Parameters	Distance from the Turbine			
[dB]	250 m	500 m	1000 m	1500 m
min	1.3	0.4	0.9	0.2
max	4.2	8.3	10.9	10.2

Table A11. Comparison of measurement and calculation results obtained using the CNOSSOS-EU model for measurement points located at different distances behind the turbine for an average wind speed of 4.6 m/s.

Distance	Indicator	Octave Band Center Frequency						
[m]	[dB]	4 Hz	8 Hz	16 Hz	31.5 Hz	63 Hz	125 Hz	250 Hz
250	$L_{p,m}$	58.1	55.2	54.2	52.2	50.6	48.8	47.4
	$L_{p,c}$	61.1	58.2	53.8	49.9	45.2	43.4	41.9
	ΔL_p	3.0	3.0	−0.4	−2.3	−5.4	−5.4	−5.5
500	$L_{p,m}$	50.3	48.4	48.6	45.6	42.4	41.4	40.4
	$L_{p,c}$	55.6	52.8	48.4	44.5	39.8	37.8	36.3
	ΔL_p	5.3	4.4	−0.2	−1.1	−2.6	−3.6	−4.1
1000	$L_{p,m}$	—	44.2	43.9	39.6	43.3	39.0	34.9
	$L_{p,c}$	49.7	46.9	42.4	38.5	33.7	31.7	29.8
	ΔL_p	—	2.7	−1.5	−1.1	−9.6	−7.3	−5.1
1500	$L_{p,m}$	46.9	41.4	40.5	36.8	38.9	29.3	27.6
	$L_{p,c}$	46.2	43.4	38.9	35.0	30.1	27.9	25.9
	ΔL_p	−0.7	2.0	−1.6	−1.8	−8.8	−1.4	−1.7

Table A12. Selected statistical parameters of the absolute values of the differences between measured and calculated values using the CNOSSOS-EU model for an average wind speed of 4.6 m/s.

Parameters	Distance from the Turbine			
[dB]	250 m	500 m	1000 m	1500 m
min	0.4	0.2	1.1	0.7
max	5.5	5.3	9.6	8.8

References

1. Krichen, M.; Basheer, Y.; Qaisar, S.M.; Waqar, A. A survey on energy storage: Techniques and challenges. *Energies* **2023**, *16*, 2271. [CrossRef]
2. Amir, M.; Deshmukh, R.G.; Khalid, H.M.; Said, Z.; Raza, A.; Muyeen, S.M.; Nizami, A.S.; Elavarasan, R.M.; Saidur, R.; Sopian, K. Energy storage technologies: An integrated survey of developments, global economical/environmental effects, optimal scheduling model, and sustainable adaption policies. *J. Energy Storage* **2023**, *72*, 108694. [CrossRef]
3. Pedersen, E.; van den Berg, F.; Bakker, R.; Bouma, J. Response to noise from modern wind farms in The Netherlands. *J. Acoust. Soc. Am.* **2009**, *126*, 634–643. [CrossRef] [PubMed]
4. Pawlaczyk-Łuszczyńska, M.; Zaborowski, K.; Dudarewicz, A.; Zamojska-Daniszewska, M.; Waszkowska, M. Response to noise emitted by wind farms in people living in nearby areas. *Int. J. Environ. Res. Public Health* **2018**, *15*, 1575. [CrossRef] [PubMed]
5. Hansen, C.; Hansen, K. Recent Advances in Wind Turbine Noise Research. *Acoustics* **2020**, *2*, 171–206. [CrossRef]
6. *ISO 7196:1995*; Acoustics—Frequency-Weighting Characteristics for Infrasound Measurements. International Standards Organisation: Geneva, Switzerland, 1995.
7. *ISO 9612:1997*; Acoustics–Guidelines for the Measurement and Assessment of Exposure to Noise in Working Environment. International Standards Organisation: Geneva, Switzerland, 1997.
8. *DIN 45680:1997-03*; Measurement and Assessment of Low-Frequency Noise Immissions in the Neighbourhood. Deutches Institut für Normung: Berlin, Germany, 1997.
9. Leventhall, G. What is infrasound? *Prog. Biophys. Mol. Biol.* **2007**, *93*, 130–137. [CrossRef] [PubMed]
10. ACGIH. *2012 TLVs and BEIs*; The American Conference of Governmental Industrial Hygienists: Cincinnati, OH, USA, 2012.
11. Berglund, B.; Hassmén, P.; Soames Job, R.F. Sources and effects of low-frequency noise. *J. Acoust. Soc. Am.* **1996**, *99*, 2985–3002. [CrossRef] [PubMed]
12. Castelo Branco, N.A. The clinical stages of vibroacoustic disease. *Aviat. Space Environ. Med.* **1999**, *70*, A32–A39. [PubMed]
13. *ANSI S12.9-Part 4-2005*; Quantities and Procedures for Description and Measurement of Environmental Sound—Part 4: Noise Assessment and Prediction of Long-Term Community Response. American National Standard, Acoustical Society of America: New York, NY, USA, 2005.
14. Pawlas, K.; Pawlas, N.; Boroń, M.; Szłapa, P.; Zachara, J. Infrasound and low frequency noise assessment at workplaces and environment—Review of criteria. *Environ. Med.* **2013**, *16*, 82–89.

15. Bertagnolio, F.; Madsen, H.A.; Fischer, A. Coupled wind turbine noise generation and propagation model: A numerical study. In Proceedings of the 7th International Conference on Wind Turbine Noise, Rotterdam, The Netherlands, 2–5 May 2017.
16. Bigot, A.; Economou, P.; Economou, C. Wind turbine noise prediction using Olive Tree Lab Terrain. In Proceedings of the 7th International Conference on Wind Turbine Noise, Rotterdam, The Netherlands, 2–5 May 2017.
17. McBride, S.; Burdisso, R. A comprehensive Hamiltonian ray tracing technique for wind turbine noise propagation under arbitrary weather conditions. In Proceedings of the 7th International Conference on Wind Turbine Noise, Rotterdam, The Netherlands, 2–5 May 2017.
18. Hansen, K.L.; Zajamšek, B.; Hansen, C.H. Investigation of a microphone height correction for long-range wind farm noise measurements. *Appl. Acoust.* **2019**, *155*, 97–110. [CrossRef]
19. Madsen, H.A.; Johansen, J.; Sørensen, N.N.; Larsen, G.C.; Hansen, M.H. Simulation of low frequency noise from a downwind wind turbine noise. In Proceedings of the 45th AIAA Aerospace Sciences Meeting and Exhibit, Reno, NV, USA, 8–11 January 2007. [CrossRef]
20. Madsen, H.A. Low frequency noise from wind turbines mechanisms of generation and its modelling. *J. Low Freq. Noise Vib. Act. Control* **2010**, *29*, 239–251. [CrossRef]
21. Ostashev, V.; Wilson, D. *Acoustics in Moving Inhomogeneous Media*; CRC Press: Boca Raton, FL, USA, 2015.
22. Barlas, E.; Zhu, W.J.; Shen, W.Z.; Dag, K.O.; Moriarty, P. Consistent modelling of wind turbine noise propagation from source to receiver. *J. Acoust. Soc. Am.* **2017**, *142*, 3297–3310. [CrossRef] [PubMed]
23. Barlas, E.; Wu, K.L.; Porté-Agel, F.; Shen, W.Z. Variability of wind turbine noise over a diurnal cycle. *Renew. Energy* **2018**, *126*, 791–800. [CrossRef]
24. Keith, S.E.; Daigle, G.A.; Stinson, M.R. Wind turbine low frequency and infrasound propagation and sound pressure level calculations at dwellings. *J. Acoust. Soc. Am.* **2018**, *144*, 981–996. [CrossRef]
25. Kelly, M.; Barlas, E.; Sogachev, A. Statistical prediction of far-field wind-turbine noise, with probabilistic characterization of atmospheric stability. *J. Renew. Sustain. Energy* **2018**, *10*, 013302. [CrossRef]
26. Cotté, B. Extended source models for wind turbine noise propagation. *J. Acoust. Soc. Am.* **2019**, *145*, 1363–1371. [CrossRef] [PubMed]
27. Bertagnolio, F.; Madsen, H.A.; Fischer, A. A temporal wind turbine model for low-frequency noise. In Proceedings of the 46th International Congress and Exposition on Noise Control Engineering (InterNoise17), Hong Kong, China, 27–30 August 2017; pp. 5025–5033.
28. Viterna, L.A. The NASA-LeRC wind turbine sound prediction code. In Proceedings of the Second DOE/NASA Wind Turbine Dynamics Workshop, Cleveland, OH, USA, 24–26 February 1981.
29. Viterna, L.A. Method for predicting impulsive noise generated by wind turbine rotors. In Proceedings of the International Conference on Noise Control Engineering (InterNoise 82), San Francisco, CA, USA, 17–19 May 1982; pp. 339–342.
30. Amiet, R.K. Acoustic radiation from an airfoil in a turbulent stream. *J. Sound Vib.* **1975**, *41*, 407–420. [CrossRef]
31. Bertagnolio, F.; Madsen, H.A.; Fischer, A. A combined aeroelastic-aeroacoustic model for wind turbine noise: verification and analysis of field measurements. *Wind Energy* **2017**, *20*, 1331–1348. [CrossRef]
32. Bertagnolio, F.; Madsen, H.A.; Fischer, A. Analysis of low-frequency noise from wind turbines using a temporal noise code. In Proceedings of the 23rd International Congress on Acoustics, Aachen, Germany, 9–13 September 2019; pp. 4414–4421.
33. Ecotière, D.; Gauvreau, B.; Cotté, B.; Roger, M.; Schmich-Yamane, I.; Nessi, M.C. PIBE: A new French project for predicting the impact of wind turbine noise. In Proceedings of the 8th International Conference on Wind Turbine Noise, Lisbon, Portugal, 12–14 June 2019.
34. Heutschi, K.; Pieren, R.; Müller, M.; Manyoky, M.; Hayek, U.W.; Eggenschwiler, K. Auralization of wind turbine noise: Propagation filtering and vegetation noise synthesis. *Acta Acust. United Acust.* **2014**, *100*, 13–24. [CrossRef]
35. Makarewicz, R.; Gołębiewski, R. The partially ensonified zone of wind turbine noise. *J. Wind Eng. Ind. Aerodyn.* **2014**, *132*, 49–53. [CrossRef]
36. Oerlemans, S.; Schepers, J.G. Prediction of wind turbine noise and validation against experiment. *Int. J. Aeroacoustics* **2009**, *8*, 555–584. [CrossRef]
37. Tian, Y.; Cotté, B. Wind turbine noise modeling based on Amiet's theory: Effects of wind shear and atmospheric turbulence. *Acta Acust. United Acust.* **2016**, *102*, 626–639. [CrossRef]
38. Buck, S.; Oerlemans, S.; Palo, S. Experimental characterization of turbulent inflow noise on a full-scale wind turbine. *J. Sound Vib.* **2016**, *385*, 219–238. [CrossRef]
39. Kayser, B.; Écotière, D.; Gauvreau, B. Criteria for the assessment of the influence of atmospheric turbulence on wind turbine noise propagation. *Acta Acust.* **2023**, *7*, 63. [CrossRef]
40. Mascarenhas, D.; Cotté, B.; Doaré, O.; Ecotière, D.; Guillaume, G.; Gauvreau, B.; Schmich-Yamane, I.; Junker, F. Wind turbine noise modeling including aeroacoustic sources and propagation effects: Comparison against field measurements. In Proceedings of the 51st International Congress and Exposition on Noise Control Engineering (INTER-NOISE 2022), Glasgow, UK, 21–24 August 2022.
41. Cotté, B.; Mascarenhas, D.; Ecotière, D.; Guillaume, G.; Gauvreau, B.; Junker, F. Validation of a wind turbine noise propagation model against field measurements. In Proceedings of the 10th Convention of the European Acoustics Association (Forum Acusticum 2023), Torino, Italy, 11–15 September 2023. [CrossRef]

42. *ISO 9613-2:2024*; Acoustics—Attenuation of Sound during Propagation Outdoors—Part 2: Engineering Method for the Prediction of Sound Pressure Levels Outdoors. International Standards Organisation: Geneva, Switzerland, 2024.
43. *Directive 2015/996*; Commission Directive (EU) 2015/996 of 19 May 2015 Establishing Common Noise Assessment Methods according to Directive 2002/49/EC of the European Parliament and of the Council. Official Journal of the European Union: Brussels, Belgium, 2015.
44. *Nordic Environmental Noise Prediction Methods, Nord2000. Summary Report. General Nordic Sound Propagation Model and Applications in Source-Related Prediction Methods*; Technical Report AV 1719/01; Delta, Danish Electronics, Light & Acoustics: Lyngby, Denmark, 2001; revised 31 May 2002.
45. *Proposal for Nordtest Method: Nord2000—Prediction of Outdoor Sound Propagation*; Technical Report AV 1106/07; Delta, Danish Electronics, Light & Acoustics: Hørsholm, Denmark, 2007; revised 13 January 2014.
46. *IEC 61400-11:2012/AMD1:2018*; Wind Turbines—Part 11: Acoustic Noise Measurement Techniques. International Electrotechnical Commission (IEC): Geneva, Switzerland, 2018.
47. Wszołek, T.; Pawlik, P.; Kłaczyński, M.; Stępień, B.; Mleczko, D.; Małecki, P.; Rozwadowski, K. Experimental Verification of Windshields in the Measurement of Low Frequency Noise from Wind Turbines. *Energies* **2022**, *15*, 7499. [CrossRef]
48. *ISO 9613-2:1996*; Acoustics—Attenuation of Sound during Propagation Outdoors—Part 2: General Method of Calculation. International Standards Organisation: Geneva, Switzerland, 1996.
49. *Directive 2002/49/EC*; Directive 2002/49/EC of the European Parliament and of the Council of 25 June 2002 Relating to the Assessment and Management of Environmental Noise. Official Journal of the European Union: Brussels, Belgium, 2002.
50. Perkins, R.; (Ed.) *A Good Practice Guide to the Application of ETSU-R-97 for the Assessment and Rating of Noise from Wind Farms*; Technical report; Institute of Acoustics: Edinburgh, UK, 2013.
51. Hart, C.R.; Reznicek, N.J.; Wilson, D.K.; Pettit, C.L.; Nykaza, E.T. Comparisons between physics-based, engineering, and statistical learning models for outdoor sound propagation. *J. Acoust. Soc. Am.* **2016**, *139*, 2640–2655. [CrossRef] [PubMed]
52. Bass, J.H.; Bullmore, A.J.; Sloth, E. *Development of a Wind Farm Noise Propagation Prediction Model*; Technical Report JOR3-CT95-0051; Joule III, Final report; The European Commission: Brussels, Belgium, 1998.
53. *ISO 9613-1:1993*; Acoustics—Attenuation of Sound during Propagation Outdoors—Part 1: Calculation of the Absorption of Sound by the Atmosphere. International Standards Organisation: Geneva, Switzerland, 1993.
54. *Directive 2021/1226*; Commission Delegated Directive (EU) 2021/1226 of 21 December 2020 Amending, for the Purposes of Adapting to Scientific and Technical Progress, Annex II to Directive 2002/49/EC of the European Parliament and of the Council as regards Common Noise Assessment Methods. Official Journal of the European Union: Brussels, Belgium, 2021.
55. Joint Research Centre and Institute for Health and Consumer Protection.; Anfosso-Lédée, F.; Paviotti, M.; Kephalopoulos, S. *Common Noise Assessment Methods in Europe (CNOSSOS-EU)—To Be Used by the EU Member States for Strategic Noise Mapping Following Adoption as Specified in the Environmental Noise Directive 2002/49/EC*; Publications Office: Luxembourg, 2012. [CrossRef]
56. Kragh, J. Nord 2000. State-of-the-art overview of the new nordic prediction methods for environmental noise. In Proceedings of the 29th International Congress and Exhibition on Noise Control Engineering, Nice, France, 27–31 August 2000.
57. Tarrero, A.; Martín, M.; González, J.; Machimbarrena, M.; Jacobsen, F. Sound propagation in forests: A comparison of experimental results and values predicted by the Nord 2000 model. *Appl. Acoust.* **2008**, *69*, 662–671. [CrossRef]
58. *Sound Propagation Modelling for Offshore Wind Farms*; Technical Report 114-362; Valcoustics Canada Ltd.: Richmond Hill, ON, Canada, 2016.
59. Panofsky, H.A.; Dutton, J.A. *Atmospheric Turbulence: Models and Methods for Engineering Applications*; Wiley: New York, NY, USA, 1984.
60. Kruskal, W.H.; Wallis, W.A. Use of ranks in one-criterion variance analysis. *J. Am. Stat. Assoc.* **1952**, *47*, 583–621. [CrossRef]
61. Kvam, P.H.; Vidakovic, B. *Nonparametric Statistics with Applications to Science and Engineering*; John Wiley & Sons, Inc.: Hoboken, NJ, USA, 2007.
62. Stępień, B. A comparison of classical and Bayesian interval estimation for long-term indicators of road traffic noise. *Acta Acust. United Acust.* **2018**, *104*, 1118–1129. [CrossRef]
63. Tukey, J.W. Comparing individual means in the analysis of variance. *Biometrics* **1949**, *5*, 99–114. [CrossRef]
64. Kramer, C.Y. Extension of multiple range tests to group means with unequal numbers of replications. *Biometrics* **1956**, *12*, 307–310. [CrossRef]
65. Howell, D.C. *Statistical Methods for Psychology*, 7th ed.; Wadsworth Publishing: Belmont, CA, USA, 2009.
66. Stępień, B. Confidence intervals for the long-term noise indicators using the kernel density estimator. *Arch. Acoust.* **2016**, *41*, 517–525. [CrossRef]
67. Spearman, C. The Proof and Measurement of Association between Two Things *Am. J. Psychol.* **1904**, *15*, 72–101. [CrossRef]
68. Myers, J.L.; Well, A.D. *Research Design and Statistical Analysis*, 2nd ed.; Lawrence Erlbaum Associates Publishers: New York, NY, USA, 2003.
69. *ISO 17534-1:2015*; Acoustics—Software for the Calculation of Sound Outdoors. Part 1: Quality Requirements and Quality Assurance. International Standards Organisation: Geneva, Switzerland, 2015.
70. *ISO/TR 17534-2:2014*; Acoustics—Software for the Calculation of Sound Outdoors. Part 2: General Recommendations for Test Cases and Quality Assurance Interface. International Standards Organisation: Geneva, Switzerland, 2014.

71. *ISO/TR 17534-3:2015*; Acoustics—Software for the Calculation of Sound Outdoors. Part 3: Recommendations for Quality Assured Implementation of ISO 9613-2 in Software According to ISO 17534-1. International Standards Organisation: Geneva, Switzerland, 2015.
72. *ISO/TR 17534-4:2020*; Acoustics—Software for the Calculation of Sound Outdoors. Part 4: Recommendations for a Quality Assured Implementation of the COMMISSION DIRECTIVE (EU) 2015/996 in Software According to ISO 17534-1. International Standards Organisation: Geneva, Switzerland, 2020.
73. Kosała, K.; Stępień, B. Analysis of noise pollution in an andesite quarry with the use of simulation studies and evaluation indices. *Int. J. Occup. Saf. Ergon.* **2016**, *22*, 92–101. [CrossRef]
74. Stępień, B. Comparison of selected methods of the confidence intervals for long-term noise indicators. *Acta Acust. United Acust.* **2017**, *103*, 339–348. [CrossRef]
75. *Directive 2020/367*; COMMISSION DIRECTIVE (EU) 2020/367 of 4 March 2020 Amending Annex III to Directive 2002/49/EC of the European Parliament and of the Council as Regards the Establishment of Assessment Methods for Harmful Effects of Environmental Noise. Official Journal of the European Union: Brussels, Belgium, 2020.

Disclaimer/Publisher's Note: The statements, opinions and data contained in all publications are solely those of the individual author(s) and contributor(s) and not of MDPI and/or the editor(s). MDPI and/or the editor(s) disclaim responsibility for any injury to people or property resulting from any ideas, methods, instructions or products referred to in the content.